Fluctuating Asymmetry and Geometric Morphometrics in A New Species of Whip Spiders (Charontidae, Amblypygi) Collected from Initao National Park, Misamis Oriental, Philippines[1]

JENEFER A. GODINEZ
MARK ANTHONY J. TORRES
CESAR G. DEMAYO

Abstract

Whip spiders belong to the less well-studied arachnid order Amblypygi. Here, fluctuating asymmetry (FA) and geometric morphometrics analyses are used as tools to assess the between-sex differences of the sampled amblypygids that are believed to belong under a new species of the Genus Charon. Metric evaluation of the structures corresponding to the left and right sides of the whip spiders was conducted through a series of tests for fluctuating asymmetry (FA) study. Results show that of the 72 traits measured, only three characters that correspond to leg 3 femur length, leg 3 patellar length and leg 4 basitibia 3 length are most ideal in FA study because they did not exhibit size dependence, antiasymmetry or directional asymmetry. Geometric morphometrics analyses using centroid size, Procrustes fitting, thin plate spline (TPS) and warps functions, Euclidean Distance Matrix Analysis (EDMA), elliptic Fourier analysis (EFA) and eigenshape analysis (EA) show that the females exhibit greater diversity in the shapes of the carapace, the sternal area and the opisthosoma of the whip spiders. Further thorough investigations on the characteristics of the samples collected from Initao National Park, Misamis Oriental have to be done to confirm whether the specimens merit a new species status.

Keywords: fluctuating asymmetry, geometric morphometrics, whip spiders, Amblypygi, *Charon*

[1] Portion of the master's thesis of JENEFER A. GODINEZ an MS Biology student, MSU-IIT. This thesis was awarded the Best Graduate Paper, MSU-IIT In-house Review 2006. MARK ANTHONY J. TORRES, Instructor, Department of Biological Sciences, MSU-IIT College of Science and Mathematics and CESAR G. DEMAYO, Professor, MSU-IIT, Department of Biological Sciences, College of Science and Mathematics.

Introduction

A whip spider is an invertebrate animal belonging to the order Amblypygi in the class Arachnida, in the subphylum Chelicerata of the Phylum Arthropoda (Farlex Inc., 2004). The amblypygids are among the least studied order of arachnids worldwide (Harvey, 2002).

Gervais first described amblypygids from the Philippines in 1842. In the section of the article "Entomologie", he named the spider *Phrynus grayi*, which was then changed to *Charon grayi*. The genus *Charon* was first recognized by Karst in 1879 (Harvey, 1998). Some time later, some more species of the same genus were described from Indonesia and New Guinea, all of which were then clumped by Kreapelin in 1895 as under the name *Charon grayi* (Weygoldt, 2002).

In Philippine setting, there is a need to update the publication about whip spiders. Two articles that date back in 1892, one by Simon and another by A. Raffray, J. Bolivar and E. Simon, described amblypygids from Luzon that were under Genus *Charon* and Genus *Sarax*. A recent publication by Weygoldt in 2002 described *Charon* specimens from Luzon and Visayas but there had never been a publication about the amblypygids from Mindanao. Therefore, it is very interesting to study the characteristics of the whip spiders specifically found in Initao National Park, Misamis Oriental, so as to provide new data that can be used for taxonomic purposes as well as to apply new approaches in the analysis of the external morphological characteristics of the whip spiders through the use of traditional and geometric morphometrics.

It is the general objective of this study to determine the between-sex differences of the whip spiders collected from Initao National Park, Initao, Misamis Oriental based on two tools fluctuating asymmetry and geometric morphometrics.

One very important impact of the study is on the biological applications of the tools used in this research. Fluctuating asymmetry (FA) had been widely used to assess the conditions of the individuals in their natural environment (Graham *et al.*, 1993). FA studies involve a series of tests where statistical algorithms are given biological meanings. Geometric morphometrics, on the other hand, as the fusion of the fields of geometry, biology and statistics, provides quantitative handling of the biologically relevant forms in order to arrive at meaningful interpretations with regards to individual variations (Oxnard, 1978). Studying variations within a species may unfold some hidden mysteries behind the organism's diversity and adaptability in coping with the conditions of the environment where they are found. Shape variations of specific structures may also be attributed to certain biological factors that had made possible such variations. Because Cartesian coordinates are used in geometric morphometric quantification of shapes instead of metric units, the effect of size, scaling and orientation of the forms are avoided using the measure of overall body size expressed in centroid size. These are only few of

the significant reasons why fluctuating asymmetry and geometric morphometrics are used in population studies.

Materials and Methods

Whip spiders were collected from the caves of Initao National Park, Initao, Misamis Oriental. Three sampling periods were done namely on January 18, 2003, October 22, 2004 and April 22, 2005. Convenient sampling of spiders was done through spotlighting in caves and hand picking the whip spiders. Sampled spiders were placed into labeled plastic containers, 5 x 8 inches in size. The sampled spiders were then placed in the refrigerator in which they quickly became quiet and soon died (Weygoldt, 2000).

The Key to the Amblypygid Genera as provided for by Weygoldt, 2000 in his book "Whip Spiders (Chelicerata: Amblypygi) Their Biology, Morphology and Systematics" was used as the basis for the classification of the whip spiders under study. Special diagnostic characters like the number of subdivisions or articles on the tibia and tarsal segments of the antenniform first pair of legs and the pedipalp spination formula were also referred to for further classification to the species level.

The differences between the left and right measurements of the 72 characters were computed to calculate for the five most frequently used FA indices (FA1, FA2, FA3, FA4 and FA5) (Palmer, 1994). Except for the number of articles on the tibia and tarsal segments of the antenniform first pair of legs, all measurements of the structures were in millimeters (mm) and were taken with the use of a Vernier caliper. Table 1 shows the summary of the 72 characters used for FA study.

A series of tests was performed using linear regression scatter plot (to take note of the distribution and the possible outliers), test for size dependence, test for Normality using Shapiro-Wilk test and the computations for skewness, Kurtosis, one-tailed t-test and Sequential Bonferroni correction.

The coordinates of the landmark and outline points on the digitized images of the dorsal carapace, the ventral sternal area and the ventral opisthosoma of the samples were determined using Scion Image software (Frederick, 2000). Geometric morphometrics analyses using centroid size, Procrustes fitting, thin plate spline (TPS) and warp functions, Euclidean Distance Matrix Analysis (EDMA), elliptic Fourier analysis (EFA) and eigenshape analysis (EA) were applied in this study. Shape differences were also evaluated using Multivariate Analysis of Variance (MANOVA), canonical variates analysis (CVA), Principal Component Analysis (PCA), Hotelling's T^2 Test and cluster analysis. The dorsal carapace and the ventral prosomal sternites on the sternal area were assigned with 12 and 26 landmark points, respectively, while the dorsal carapace and the ventral opisthosoma were assigned with 44 and 56 outline points, respectively. Figures 1, 2 and 3 show the landmark points (designated with numbers, with corresponding

descriptions of anatomical locations in Tables 2 and 3) and outline points (red marks) assigned to the chosen structures.

Data analyses were performed using computer programs such as the Microsoft Excel, Analyze It software, and PAST (PAleontological STatistics, version 1.27) (Hammer *et al.*, 2004) software.

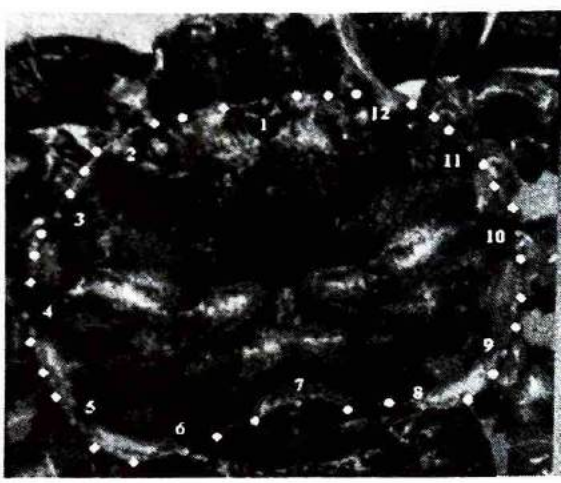

Figure 1. Locations of the carapace landmark (red) and outline (yellow) points.

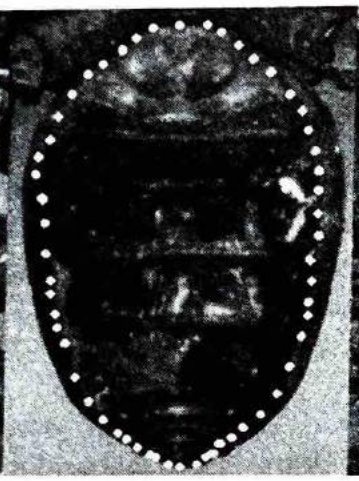

Figure 2. Outline points (yellow) on the ventral opisthosoma.

Figure 3. Landmark Points (red) on the Ventral Prosoma, along the sternal area.

Table 1. Summary of the 72 characters measured for FA study

NUMBER	CHARACTER DESCRIPTION
	Eyes
1	LME (left median eye) diameter
	RME (right median eye) diameter
2	LLE (left lateral eye group) diameter
	RLE (right lateral eye group) diameter
3	Distance between LLE and LME
	Distance between RME and RLE
4	Lateral eye to anterior edge (left side)
	Lateral eye to anterior edge (right side)
5	Lateral eye to lateral edge (left side)
	Lateral eye to lateral edge (right side)
	Chelicerae
6	Left chelicerae basal article
	Right chelicerae basal article
7	Left chelicerae terminal article (fang)
	Right chelicerae terminal article (fang)
8	Total cheliceral length (left)
	Total cheliceral length (right)
	Pedipalps
9	Left Coxa
	Right Coxa
10	Left trochanter length
	Right trochanter length
11	Left trochanter width
	Right trochanter width
12	Left femur length
	Right femur length
13	Left femur width
	Right femur width
14	Left patella length
	Right patella length
15	Left patella width
	Right patella width
16	Left tibia length
	Right tibia length
17	Left tibia width
	Right tibia width
18	Left claw
26	No. of subdivisions on left tarsus
	No. of subdivisions on right tarsus
27	Total length of left leg 1
	Total length of right leg 1
	Leg II
28	Left Coxa
	Right Coxa
29	Left Trochanter
	Right Trochanter
30	Left Femur
	Right Femur
31	Left Patella
	Right Patella
32	Left Basitibia
	Right Basitibia
33	Left Distitibia
	Right Distitibia
34	Left Basitarsus
	Right Basitarsus
35	Left Telotarsus
	Right Telotarsus
36	Left Apotele
	Right Apotele
37	Left Tarsal claw 1
	Right Tarsal claw 1
38	Left Tarsal claw 2
	Right Tarsal claw 2
39	Total tarsal length (left) 1
	Total tarsal length (right) 1
40	Total tarsal length left 2
	Total tarsal length right 2
41	Total left leg 2 length w/o claw
	Total right leg 2 length w/o claw
	Leg III
42	Left Coxa
	Right Coxa
43	Left Trochanter

	Right claw		Right Trochanter
19	Total Left Pedipalp Length	44	Left Femur
	Total Right Pedipalp Length		Right Femur
	Leg I	45	Left Patella
20	Left Coxa		Right Patella
	Right Coxa	46	Left Basitibia
21	Left femur		Right Basitibia
	Right femur	47	Left Distitibia
22	Left patella		Right Distitibia
	Right patella	48	Left Basitarsus
23	Left tibia		Right Basitarsus
	Right tibia	49	Left Telotarsus
24	Left tarsus		Right Telotarsus
	Right tarsus	50	Left Apotele
25	No. of subdivisions on left tibia		Right Apotele
	No. of subdivisions on right tibia		

Table 1. Summary of the 72 characters measured for FA study (Cont.)

NUMBER	CHARACTER DESCRIPTION	NUMBER	CHARACTER DESCRIPTION
51	Left Tarsal claw 1	62	Left Basitibia 3
	Right Tarsal claw 1		Right Basitibia 3
52	Left Tarsal claw 2	63	Left Basitibia 4
	Right Tarsal claw 2		Right Basitibia 4
53	Total tarsal length (left) 1	64	Left Distitibia
	Total tarsal length right 1		Right Distitibia
54	Total tarsal length (left) 2	65	Left Basitarsus
	Total tarsal length right 2		Right Basitarsus
55	Total left leg 3 length w/o claw	66	Left Telotarsus
	Total right leg 3 length w/o claw		Right Telotarsus
	Leg IV	67	Left Apotele
56	Left Coxa		Right Apotele
	Right Coxa	68	Left Tarsal claw 1
57	Left Trochanter		Right Tarsal claw 1
	Right Trochanter	69	Left Tarsal claw 2
58	Left Femur		Right Tarsal claw 2
	Right Femur	70	Total tarsal length (left) 1
59	Left Patella		Total tarsal length (right) 1
	Right Patella	71	Total tarsal length (left) 2
60	Left Basitibia 1		Total tarsal length (right) 2
	Right Basitibia 1	72	Total left leg 3 length w/o claw
61	Left Basitibia 2		Total right leg 3 length w/o claw
	Right Basitibia 2		

Table 2. Landmark Points and Their Corresponding Anatomical Locations on the Dorsal Carapace

LANDMARK NUMBER	ANATOMICAL LOCATIONS ON DORSAL CARAPACE
1	Anterior margin directly above the center of the two median eyes
2	Left lateral margin of the anterior region of the carapace
3	Slight depression at the antero-lateral margin near the left lateral eye triad
4	Shallow curved groove along the left lateral margin of the carapace
5	Convex curve at the left postero-lateral margin of the carapace
6	Convex curve at the left posterior margin of the carapace
7	Depression at the middle of the posterior margin
8	Convex curve at the right posterior margin of the carapace
9	Convex curve at the right postero-lateral margin of the carapace
10	Shallow curved groove along the right lateral margin of the carapace
11	Slight depression of the antero-lateral margin near the right lateral eye triad
12	Right lateral margin of the anterior region of the sample

Table 3. Landmark Points and Their Corresponding Anatomical Locations on the Ventral Prosoma, along the Sternal Area

LANDMARK NUMBER	ANATOMICAL LOCATIONS ON THE VENTRAL PROSOMA
1	Tip of the tritosternum
2	Ventral base of the tritosternum, right side
3	Posterior base of the tritosternum along the midpoint of the right pedipalp coxa
4	Point between right coxa and leg 1
5	Sternal area between right leg 1 and leg 2
6	Mid-sternal section of the right leg 2
7	Sternal area between right leg 2 and leg 3
8	Mid sternal section of the right leg 3
9	Base of the projecting structure between right leg 3 and leg, along leg 3
10	Tip of the projecting structure, right side
11	Base of the projecting structure between right leg 3 and leg 4, along leg 4
12	Mid-sternal section of the right leg 4
13	Sternal area between right leg 4 and the stalk or petiolus
14	Mid-sternal section of the stalk or petiolus
15	Sternal area between left leg 4 and the stalk or petiolus
16	Mid-sternal section of the left leg 4
17	Base of the projecting structure between left leg 3 and leg 4, along leg 4
18	Tip of the projecting structure, left side
19	Base of the projecting structure between left leg 3 and leg, along leg 3
20	Mid-sternal section of left leg 3
21	Sternal area between left leg 2 and leg 3
22	Mid-sternal section of the left leg 2
23	Sternal area between left leg 1 and leg 2
24	Point between left coxa and leg 1
25	Posterior base of the tritosternum along the midpoint of the left pedipalp coxa
26	Ventral base of the tritosternum, left side

Results and Discussion

Twenty-three females (1F to 23F) and eleven males (1M to 11M), for a total of 34 whip spiders were collected after three sampling periods. Based on the available identification key for amblypygid genera, the samples, having pedipalp tibia with two large dorsal spines followed distally by a distal reduced spine but without articulation between pedipalp distitarsus and its terminal claw, can be classified under genus *Charon*. Examination of the species-specific number of articles in the tibia and tarsus of the first pair of legs revealed that the samples from Initao National Park, Misamis Oriental have 18-38 articles and 17-48 articles on the tibia and tarsus, respectively. The difference in the number of articles from the diagnostic character of only 25 articles on the tibia and only 44-45 articles in the tarsus make it possible that the specimen belong under a new species of genus *Charon*.

The lengths of the four pairs of legs of the 34 specimens were compared to get the leg formula of the whip spiders. The leg formula is designated by numerals 1, 2, 3 and 4 for the first, second, third and fourth pair of legs, respectively, and then by arranging the lengths of the legs in descending order. There were three leg formulae that were derived from the lengths of the legs of the samples. A total of 12 whip spiders, with 7 females (1F, 7F, 9F, 12F, 13F, 18F and 20F) and 5 males (2M, 3M, 5M, 8M and 10M), exhibit a leg formula of 1>4>3>2. There were eight whip spiders that exhibit a leg formula of 1>3>4>2. Among them were six females namely, 2F, 3F, 4F, 16F, 21F and 23F; and, only two males 4M and 6M. Only one sample exhibited a leg formula of 1>4>2>3 and this is specimen 6F. A unique formula formulated in this study can be explained to as leg 1 being the longest, followed by the approximate but not equal lengths of any of the left and right sides of legs 3 and 4 and followed by legs 2 being the shortest of the four legs. This is shortened here as $1>3\approx\neq4>2$ which are exhibited by six females (5F, 14F, 15F, 17F, 19F and 22F) and three males (7M, 9M and 11M). There were four specimens (three females namely, 8F, 10F and 11F; and, one male, 1M) with a leg that is either cut or missing and so their leg formulae cannot be distinguished.

The literatures have been surveyed for the possible reasons why the whip spiders have obvious deviations from the right and left lengths of their legs and for why they have varied leg formulae. One intrinsic characteristic of amblypygids is that they are capable of autotomy and regeneration with the breaking plane is at the patella-tibia point, which is almost immovable in all legs, and that serves apparently only for autotomy (Weygoldt, 2000) can be one of the reasons for the observed deviations.

According to Weygoldt (2000), the autotomy in whip spiders is an active process and not just done by simply rupturing the joint membranes between patella and tibia. Weygoldt explains further that the physiological explanation is the presence of the three muscles: the first is attached at the distal part of the femur, the second at the dorsal and anterior sides of the patella and the third at the breaking plane on the tibia. The breaking zone detaches when all three muscles contract suddenly, in such a way that when

the spider is held in any of its legs such that the tibia is squeezed, it can break off its tibia in order to escape. It can even break off the injured tibia by itself and autotomize it later. However, if the femur is cut, the leg will not be regenerated (Weygoldt, 2000). Even if only any of the distal part of the legs (such as the tarsus) is cut off, the remaining tibia has to be autotomized before regeneration occurs during the intermolt stage; and, there is no visible regeneration bud on the outside but after molting, the regenerated leg is complete and functional, but it may differ to the usually larger non-generated leg on the other side (Weygoldt, 2000). A regenerated leg 4, for instance, may exhibit an unusual basitibia. Therefore, autotomy is one reason for the variation in leg formulae.

The articles on the whip-like first pair of legs are most easily cut and newly generated antenniform legs are shorter by about two-thirds than the intact counterpart on the other side; however, the relatively shorter articles may be increased in number by about 30% on its tarsus and up to 60% on its tibia (Weygoldt, 2000). Other observable features on a regenerated antenniform leg are the incompletely separated articles and the varying irregular lengths of each article. At subsequent molts, the number of articles and the other features remain constant; however, the articles extend making the regenerated antenniform leg eventually longer than its original counterpart (Weygoldt, 2000).

Another "species-specific" character is the number of spines on the pedipalp, specifically the number of spines on each of the articles of the pedipalp.

The pedipalp spination of the three new species from Australia discovered by Harvey (1998) varies greatly with that observed on the samples examined as representatives for the population in Initao National Park. There are more than 4 species of *Charon* (Weygoldt, 2000) but from the review of specimen mentioned in the paper of Harvey (1998), there may be around 10 *Charon* species so far. In Table 4, the data on the spine formulation both the dorsal and ventral sides of the articles of the pedipalp of the samples from Initao National Park are compared with those of the three new species discovered by Harvey (1998) from Australia. Upon examination of the data in Table 4, there are no other similarities observed to be common with the identified species, other than the diagnostic feature of the *Charon* having three spines on the pedipalp tibia, the 1st reduced spine and two long spines. It can also be observed that the spination on the trochanter, femur and patella of the first three species discovered by Harvey in Australia significantly differ from the *Charon* species collected from Initao National Park, Misamis Oriental. Only in the number of spines in the tibia of *Charon gervaisi* do the *Charon* species from Initao have similar observable pedipalp spination. For this reason, the researcher strongly believes that a much thorough investigation of the pedipalp spination may lead to the confirmation of a novel species of *Charon*. Moreover, there is a need to compare the collected data of the whip spiders sampled here with the other species already identified and most especially with the type specimens collected by Gervais from the Philippines in 1842 and with those that were collected and published by Weygoldt in 2000.

Table 4. Summary of the Pedipalp Spination of the *Charon* species collected from Initao National Park, Misamis Oriental compared to the three Australian species discovered by Harvey (1998).

NEW SPECIES (Harvey, 1998)	SPINATION ON THE PEDIPALP ARTICLES			
	Trochanter	**Femur**	**Patella**	**Tibia**
Charon oenpelli	D3-7 V3-14	D9-31 V9-32	D8-31 V11-29	D3-12 V2-11
Charon trebax	D8 V4	D16 V14	D15 V19	D3 V3
Charon gervaisi	D5-7 V6-7	D14-20 V17-20	D17-22 V16-19	D 2-3 V2
Charon species *(from Initao)*	D11-13 V9-12	D6 V7	D5 V6	D3 V2

Legend: D = dorsal view; V = ventral view

When taking two linear measurements, it can sometimes be found that the ratio between them remains constant such that the shape stays the same and this is called *isometric* growth, meaning that growth rate is the same everywhere (homogenous) and the same in all directions (isotropic); but, it is more commonly seen that the ratio between the measurements changes systematically upon growth and development giving a continuous change in proportion and this is known as *allometric* growth (Hammer *et al.*, 2004). A well-known example of allometric growth is head size in humans and many other vertebrates. The head grows slower than the rest of the body, giving a diminishing ratio between head and body size as the child matures. Is allometry present in whip spiders?

Of the 72 characters tested for size-dependence, only two character traits showed significant results at the significance level of 0.05 and these are character 14 (pedipalp patella length) and character 19 (total pedipalp length) with p(uncorr) values of 0.00025197 and 0.01698, respectively. These two traits that show size dependence also exhibit negative slope. This further means that as the body size increases, the length of the pedipalp patella greatly decreases and so the total length of the pedipalp also decreases. Thus, this linear relationship of the spider length and the lengths of pedipalp patella is an example of allometry. Figure 4 below shows the scatter plot of these two characters.

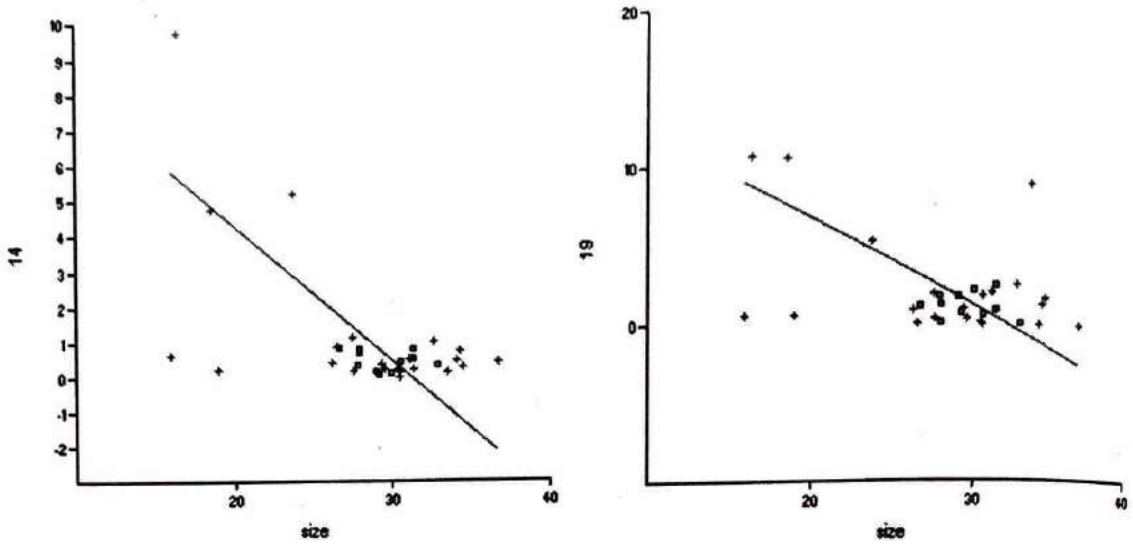

Figure 4. Scatter plot showing the linear relationship of the characters with the body size (**14.** p=0.00025197; **19** p=0.01698).

Many statistical tests assume that the data are normally distributed (follow the "bell" or "Gauss" curve) but this is not always the case. That is why there is a need for testing for Normality in order to determine whether the values are indeed normally distributed. The normal distribution has two parameters: the *mean* and the *variance*. The variance indicates the width of the bell curve. There are several available tests for normal distribution. Using PAST, the good test with high power called Shapiro-Wilk, which is optimized for small sample sizes (N<50), is used in this study (Hammer, 2002).

Traits exhibiting significant departures from normality should be viewed with caution as valid FA that is to be used as a measure of developmental stability because they do not conform to the pattern of bilateral variation expected due to developmental noise that is viewed as a cumulative consequence of the random variation in the different developmental processes that affect each side independently (Palmer, 1994). Therefore, the traits that exhibit significant departure from normality, just like through the Shapiro-Wilk test used in this study, should be excluded from the studies of developmental stability. Among the 72 characters of the whip spiders studied that are not "ideal" to be included as in FA studies are the traits 2, 3, 4, 6, 8, 9, 10, 15, 16, 18, 21, 22, 23, 24, 27, 28, 29, 30, 32, 33, 34, 35, 37, 38, 40, 41, 42, 43, 48, 49, 50, 51, 52, 53, 53, 56, 57, 58, 59, 65, 66, 67, 68, 69, 70, 71 and 72. Any of these traits, however, can still be used for FA study provided that size dependence, skewness, antiasymmetry and directional asymmetry are absent.

Frequency distributions of R-L may depart from normality in several ways, including a skew (a long tail on one side), leptokurtosis (narrow peak and long-tailed) and platykurtosis (broad peaked and short-tailed, bimodal) (Palmer, 1994). FA studies yield results that are leptokurtic and ideally with R-L=0 and with normal variation. This is the reason why the false assumption of a normal distribution to *always* exhibit symmetry has to be

discarded because a population of bilateral individuals may also exhibit normal distribution curve even when they experience FA (Palmer, 1994).

Frequency distributions usually exhibit one of the three patterns of common distributions in bilateral organism, namely fluctuating asymmetry (FA), directional asymmetry (DA) and antiasymmetry that is platykurtic and bimodal (Palmer, 1994). In this study, DA was tested.

DA can be tested by the presence of a significant p value of the one-tailed t test. One-sample t-test giving significant p value shows directional asymmetry (DA) for traits 7, 25, 29, 32, 41 and 60.

Antiasymmetry is determined by the negative Kurtosis coefficient and a mean that is normally zero. A significant result based on the p value of skewness signifies that the data points are distributed in such a way that they are inclined to one side or are skewed either to the left or to the right. Significantly skewed characters are those numbered 1, 7, 8, 11, 17, 19, 20, 22, 25, 26, 29, 30, 33, 36 and 39. Antisymmetry was also tested.

A negative sign on the value of the Kurtosis coefficient signifies that the distribution is platykurtic or that it is broad-peaked, short-tailed and bimodal, thus exhibiting antiasymmetry. The traits 3, 9, 10, 15, 18, 21, 27, 28, 30, 32, 37, 41, 42, 43, 48, 50, 51, 52, 53, 54, 57, 65, 67, 69 and 72 exhibit antiasymmetry.

Tests for the presence of directional asymmetry and antiasymmetry in the studies of FA are done for two reasons. First, the presence of DA artificially inflates the values of certain FA indices. Second reason is that if a trait exhibits DA, some portion of the between-sides variation may have a genetic basis, hence the between-sides variance may not purely be a product of developmental noise (Palmer, 1994).

Fluctuating asymmetry (FA) describes patterns of variation in the natural environment. FA as a pattern of between-sides variation in a sample of individuals is a reflection of the developmental compromise between two processes of developmental noise (also known as developmental instability) versus developmental stability (Palmer, 1994). Developmental noise refers to the processes that tend to disrupt the precise development, as such these include: the small, random differences in rates of cell division, cell growth and cell shape change; the effect of thermal noise on the enzymatic processes; and, the small random differences in the rates of physiological processes among cells (Palmer, 1994). Developmental stability, on the other hand, refer to the processes that tend to resist or buffer the disruption of precise development that includes any of the: negative feedback systems that regulate enzyme activity (both concentration and catalytic rates) within and between cells; central nervous regulation of non-contiguous structures; or, hormonal regulation of non-contiguous structures (Palmer, 1994). In this research, the FA in whip spiders was studied.

The relevance of the skewed or leptokurtic (long-tailed) distributions of the R-L to studies of FA is somewhat less clear though it may also signal the presence of a genetic component to subtle asymmetries (Palmer, 1994). The common source of skew or leptokursis is outliers that can deviate the distribution unusually far from zero. Such deviations could either be due to

measurement errors (which is not true in this study because proper care was taken to ensure that measurement errors are avoided, such that remeasurements were done) or they might reflect truly unusual deviation from symmetry due to prior injury or trauma (Palmer, 1994). If the latter was suspected, such individuals were excluded from the FA study part of this research.

When a large number of traits have been analyzed in a single study, care must be taken in order not to be misled by "false" significant results by computing for the Sequential Bonferroni correction (Palmer, 1994). It is the usual practice that given a significance level of 0.05, when the p is less than this, with completely random data, the test yields a "significant" result. However, when there are a lot of traits studied, e. g. 8 or more (Palmer, 1994), "false positive tests" may arise. In order to avoid wrong interpretation of the analyzed data due to "false positive results," the Sequential Bonferroni correction was conducted here.

After conducting the Sequential Bonferroni correction for the p values of the coefficients for skewness, only three characters remain to have significant p values (from the 15 characters that previously showed significant p values using univariate analysis) and these are traits 19, 25 and 26. All the other 12 characters give "false" positive results. Another interesting result is that there are characters that showed not significant result in the initial univariate analysis, yet they have become significant after Bonferroni correction. These are characters 12, 14, 47, 58, 60, 61 and 13. Therefore, not only will the Bonferroni correction test for "false" positives, but they can also identify "false" negative results that can after sequential Bonferroni correction become included among the characters that exhibit skewness. Moreover, because traits 19, 25 and 26 gave consistently positive results in both the p values of the descriptive univariate analysis and the Sequential Bonferroni correction, the three traits are the true characters that indeed exhibit skewness to one side, that is, they are all skewed to the right.

There are only 11 traits that show significant results for the revised probability values after Sequential Bonferroni correction for multiple of the p value of the Kurtosis traits at 0.05 level of significance. These characters are 12, 14, 47, 58, 13, 25, 26, 61, 63, 64 and 31 where the first four characters (12, 14, 47 and 58) are also highly significant for having a positive result at 0.01 level of significance. All of these eleven traits yield "not significant" results before the Bonferroni correction of the p value. It can be inferred, then, that all 11 traits gave "false" negative results in the initial univariate test. It can also be recalled that there were 26 traits that exhibit antiasymmetry due to the negative value of the Kurtosis coefficients. Because these 26 traits did not show negative results after Sequential Bonferroni correction, they then gave "false" positive results in the initial test before Bonferroni correction.

Only one character (character 9 that corresponds for the left and right coxae of the pedipalp) gives a true conclusion of a significant result of the test for directional asymmetry (DA) at the alpha confidence level of 0.05. It is amazing to note also that trait 9 gave a "not significant" p value result of initial t test before Bonferroni correction, yet it becomes the only true positive

result after the Sequential Bonferroni correction. Traits 41, 25, 29, 32, 60 and 7 that showed positive results in the initial t-test are "false" positive results that are affected by the multiple traits studied here.

Many different indices have been used to describe the level of FA in a population. The indices differ in the degree to which they may be biased by overall trait size variation, by the presence of DA and antiasymmetry and by departures from normality of the frequency distribution of R-L (Palmer, 1994). Any of these indices is sensitive to either antiasymmetry or DA, or both. This is why the tests for the presence of antiasymmetry and DA were done prior to the computation of the FA indices. Because indices also differ in their sensitivity to other factors like trait size variation, outliers and other departures from normality, it had always been the practice that at least two FA indices are used in the tabulation of FA to illustrate the dependence of differences in FA of the choice of index (Palmer, 1994). In this study, five FA indices were used.

The absolute values and signed values of the differences between the right and left measurements of the 72 characters of the whip spiders were examined to come up with the computations of five FA indices used in this study, namely FA1, FA2, FA3, FA4 and FA5. The first three indices FA1, FA2 and FA3 are computed from the unsigned (absolute) symmetry |R-L| while the other two indices FA4 and FA5 deal with signed asymmetry (R-L) (Palmer, 1994).

The males and females showed varying degrees of fluctuation. There are 30 characters, comprising about 42% of the 72 characters that show that the females exhibit greater FA indices than the males that exhibit greater FA indices over the females only in 19 characters (26% of 72). The rest of the characters such as the eyes, pedipalps and each of the four pairs of legs showed varying FA indices for both the female and male whip spiders. The males have predominantly greater FA indices than the females based on the measurements of the cheliceral characters. However, the chelicerae have the least number of only three characters examined. On the other hand, the females exhibit relatively higher FA indices on the pedipalps since of the 11 pedipalpal characters, only on the trochanter lengths and widths do the males exhibit greater FA indices than the females, but the females predominated over the rest of the nine characters. The possible explanation for this is that this may have something to do with the stress the muscular trochanters of the male exert in holding the femur up during hunting and in courting (Weygoldt, 2000). A better and more conclusive explanation could have been gathered if there were more male samples collected.

In general, the FA indices differ in the degree at which they are biased by overall trait size (size dependence), by the presence of DA and antiasymmetry and by the departures from normality of the frequency distribution, particularly that they are most especially biased by the presence of outliers. In order to better evaluate the FA indices, the researcher had summarized the factors that can affect the degree of how each of the five indices could be biased by the presence ("yes") and the absence ("no") of such factors (Table 5).

The presence and absence of size dependence, DA and antiasymmetry had been conducted in this research to assess as to which of the FA indices are applicable to each of the 72 measured characters. All the indices are greatly biased by the presence of antiasymmetry so that characters exhibiting antiasymmetry, such as 12, 13, 14, 25, 26, 31, 47 and 58 are not suitable for FA studies. So do the structures with the presence of DA, such as character 9, so it is also not suitable for FA study.

Table 5. Summary of the presence or absence of the factors that can affect the validity of the indices to be used in FA studies

FA INDICES: FORMULA	ANTIASYMMETRY	DA	SIZE DEPENDENCE
FA1: mean |R-L|	no	no	no
FA2: mean [|R-L|/ ((R+L)/2)]	no	no	yes
FA3: mean |R-L|/ mean((R+L)/2)	no	no	yes
FA4: var(R-L)	no	yes	yes/no
FA5: $\Sigma(R-L)^2/N$	no	no	yes/no

For those characters that initially show significant p values on the tests for skewness, negative kurtosis and DA **before** Sequential Bonferroni correction, and at the same time did not show normal distribution in the Shapiro-Wilk test, may still be considered as characters for this FA study but care must be taken in the interpretation such that the initial significant p values should be noted. Interpretation must be done then with great care for characters 1, 3, 5, 7, 8, 10, 11, 15, 17, 18, 20, 21, 22, 27, 28, 29, 30, 32, 33, 36, 37, 39, 41, 42, 43, 46, 48, 50, 51, 52, 53, 54, 55, 57, 65, 67, 69 and 72. Interpretation for character 60 also needs to be done with skeptism because it is skewed to the right.

Of the two characters that yielded positive results for size dependence, character 14, which corresponds for pedipalp patella, also exhibits antiasymmetry; and, character 19, which corresponds for total pedipalp length that is also skewed to the right. These two traits are not suitable to be used for FA study because both 14 and 19 greatly affected the values for FA1 and that 14 in particular made all the other indices biased due to the presence of antiasymmetry.

Of all the 72 characters measured in this study, only three traits exhibit characteristics that can be considered as **most ideal** after all the series of tests done for the FA part of this research (Figure 5). These are characters

44, 45 and 62 that correspond for leg 3 femur length, leg 3 patellar length and leg 4 basitibia 3 length, respectively.

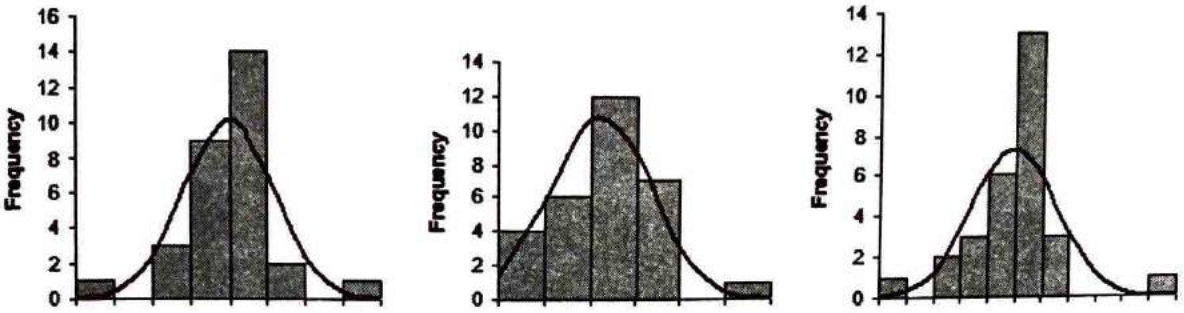

Figure 5. The descriptive frequency distribution of the character (a) 44, (b) 45 and(c) 62 that are most ideal for FA study.

Characters 44, 45 and 62 are considered most ideal because they showed positive results in the Shapiro-Wilk test for normal distribution yet did not show significant results for all the tests for size dependence, skewness, DA and antiasymmetry, both before and after the Sequential Bonferroni correction. FA1, FA2, FA4 and FA5 are the applicable indices for these characters.

The five FA indices differ on the form of size correlation whether *by individuals* in the population (FA2), *by samples of population* (FA3) or by which there is *no correlation* (FA1, FA4 and FA5) (Palmer, 1994).

The individuals sampled in this study are taken to be under the same species so that they all belong in one and the same population, so FA3 is not applicable in this study. However, it is still included in the analysis here for the purpose of comparison. Moreover, the names and the respective formulae assigned to each of the FA indices are based on international convention so if FA3 was previously excluded from this study, the readers may wonder why FA3 is missing or skipped from the analysis. These are the reasons why FA3 is still included here even when it is not recommendable to be used because there is only one sampled population dealt with in this research.

FA4, on the other hand, is a useful descriptor of FA but it is sensitive to outliers (Palmer, 1994). So, for the characters that show **outliers** in their scatter plots (such as characters 4, 23, 38, 40, 68, 70 and 71), only FA1, FA2 and FA5 are the FA indices recommended to be used. FA4 is not included among the recommended FA indices because FA4 is biased by the presence of the outliers. FA1, FA2, FA5 and FA4 are recommended in characters 2, 6, 16, 24, 34, 35, 49, 56, 59 and 66 because they did not exhibit outliers in their scatter plots.

Of the three recommended FA indices (FA3 being excluded and FA 4 being sensitive to outliers), **FA2** is the most appropriate FA index to be used in this study based on the form of correlation which is *by individuals* in just one population collected from Initao National Park, Misamis Oriental.

Because x and y coordinates of the landmark and outline points are used in the study, instead of metric units, to estimate size, the size factor from an object description is eliminated. Instead, a *centroid size*, which is the sum of the squared distances between all landmarks (Pavlinov, 2001), gives a measure of overall body size. Hammer *et al.* (2004) also defines centroid size as the Euclidean norm of the distances from all landmarks to the centroid. The PAleontological STatistics (PAST) software was used in the calculation of the centroid sizes of the carapace, the sternal area and the opisthosoma of the whip spiders sampled and analyzed in this research.

Univariate analysis using the box plot of the centroid sizes of the carapace, the sternal area and the opisthosoma are shown in Figure 6. The red boxes represent the females and the blue boxes correspond for the males. The 25 to 75 percent quartiles of the centroid sizes are drawn inside the boxes. The median is shown with a horizontal line inside the box and the minimal and maximal values of the centroid sizes are shown with short horizontal lines or "whiskers".

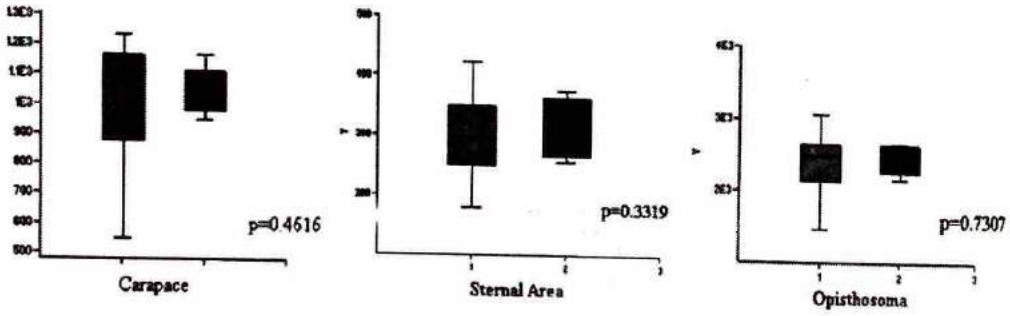

Figure 6. Box plot of the centroid sizes from the landmark and outline points on the carapace, the sternal area and the opisthosoma of the male (blue box) and female (red box) whip spiders. (Black line within each box signifies the median of the centroid size.)

Shape is a function of the relative positions of the morphological landmarks and outlines that consist of coordinates that are invariant to the effects of size, location and orientation of an object (Rohlf, 2002). One can study the differences in shapes using any of the landmark methods that belong to three broad classes, namely: superimposition methods that determine form change by the displacements of landmarks along the same coordinate space; deformation methods that make use of deformation technique for the demonstration of the difference between forms; and, linear distance-based methods that connect landmark pairs with the corresponding linear distances (Richtsmeier *et al.*, 2002). Examples of the superposition method and deformation methods are the Procrustes analysis and the thin plate spines (TPS) and warp functions, respectively. An example of the linear distance-based method, on the other hand, is the Euclidean Distance Matrix Analysis or EDMA.

Superimposition methods, like the Procrustes analysis, commonly remove or eliminate the differences in rotation, translation and scaling of forms and these methods are useful because they produce a clear graphic output that allows form or shape differences to be illustrated as absolute displacements of landmarks (Richtsmeier *et al.*, 2002). Figures 7 and 8 show the comparison of the landmark plots of the coordinates digitized form the carapace and the sternal area, respectively.

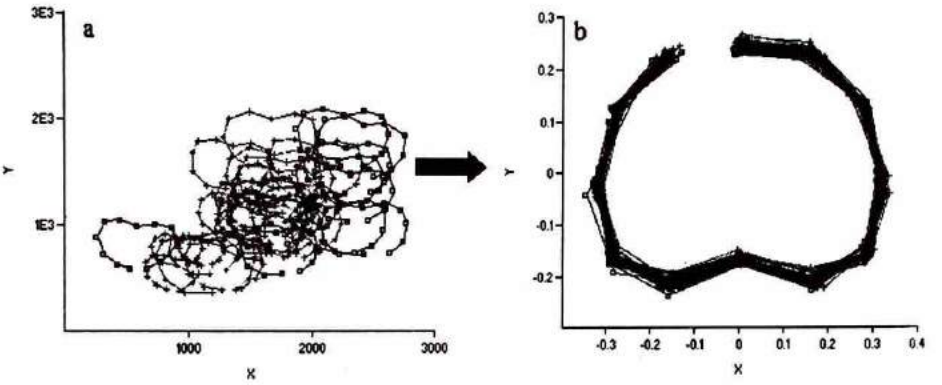

Figure 7. Comparison of landmark plots of the coordinates digitized from the carapace (a) before and (b) after Procrustes superimposition.

It can be observed on Figure 7a that except for one male (specimen 2M), the carapace plots of most males and all the females are gathered at similar axes on the plot, such that the coordinates of the landmarks of the males fall around and above the 2000 mark on the x-axis while those of the females fall around and below the 2000 mark on the x-axis. In Figure 7b, however, the landmark plots do not show great difference after Procrustes superimposition. Procrustes superimposition is used to give a generalized shape of the structures subjected to landmark analysis since the samples do not exhibit an alignment that is fit to be considered as its general form without the effect of size and orientation (Hammer, 2002). Procrustes fitting is an important procedure because it removes variation in digitizing condition, orientation and scale and superimposes the samples in common (though arbitrary) coordinate system (Hammer *et al.*, 2004).

Figure 8 shows an interesting landmark plot of the sternal area coordinates. In Figure 8a, the landmark plots for the males are gathered around and above the 2000 mark of the x-axis while those of the females fall near and below the same 2000 mark. Unlike Figure 7a, none of the samples are separated from the range where the plots of the samples of the same sex are grouped or concentrated. Looking at the superimposed plot of the landmarks after Procrustes fitting, however, a thick and seemingly disorganized sketch is formed. The plot is disorganized in such a way that the common spots of the specific landmark numbers cannot be deciphered. This implies an erratic displacement of the landmark points, as can be exhibited by their deformations.

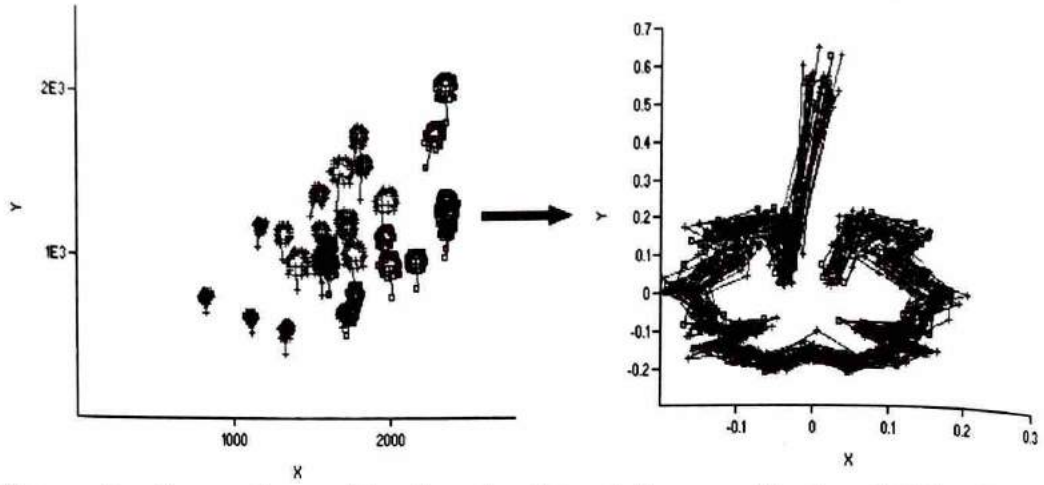

Figure 8. Comparison of landmark plots of the coordinates digitized from the sternal area (a) before and (b) after Procrustes superimposition.

If Procrustes fitting is under the superimposition methods, thin-plate spline (TPS) is an example of a deformation technique that uses chosen functions to map the relative position of points in the initial original configuration to the corresponding locations with those with deformations due to specific parameters like the bending energy within the function (Richtsmeier *et al.*, 2002). The bending energy coefficients numerically estimates the degree of smooth deformation on a thin homogeneous deformable metallic plate where each object is fit so that TPS analysis of the shapes of the structures can be compared (Pavlinov, 2001). TPS can be used to represent shape differences as smooth deformations of the mean shape into another shape (Rohlf, 2002). If one imagines a surface as a thin metal plate that will take the shape of the object fit on it, it bends as the landmark point is displaced from the mean value, such deformation can be exhibited by the change in the appearance of the grids. The more differences among shapes in the vicinities of a landmark on the transformation grid, the more the deformation of the respective fragment of the grid (Pavlinov, 2001).

Based on the carapace shape of the specimens, most females have carapace that are longer than wide while the males mostly have wider than long carapace. This statement needs further investigation in future studies, however, using a greater number of amblypygid samples, in order for it to be conclusive.

To better determine the shape variation within samples and to generate variables from shape spaces, the partial warp analysis is used to describe the major trends in deformation that can be localized on the body of the organism.

Deformation may either be affine or non-affine. Affine (uniform) deformation requires zero bending energy whereas the non-affine or non-uniform components of change require successively larger amounts of bending energy at successively smaller, more local scales of deformation (Lynch *et al.*, 1996). This means that a greater amount of bending energy is

needed to deform the shape by moving two landmarks that are close to each other than to move landmarks that are relatively separated from each other. In Figure 9, the carapace shape with the label "affine" shows the mean shape of the carapace of the whip spiders for comparison with the partial warp 1 to 9 deformation grids.

Using partial warps, any deformation of the structure shape can better be evaluated through the use of the transformation grids fit on the background of the shape. These are helpful even when only subtle shape differences are observable. The differences in the deformation grids fitted at the background of the shapes of the structures can easily be detected whether they exhibit expansion or stretching, contraction or compression or even the slight deformations along each of the partial warps. Any difference in shape, even when they are small or hard to see, can be exaggerated by increasing the amplitude of the degree of deformation from the affine or uniform component with an amplitude equal to zero to a maximum of amplitude 10 that exhibit the greatest extent of deformation. To determine the trend in the variations of the partial warps, from warp 1 to warp 9 of the carapace, Figure 9 shows the grid deformations at the maximum amplitude of 10 as compared to that of the affine or mean shape at amplitude 0.

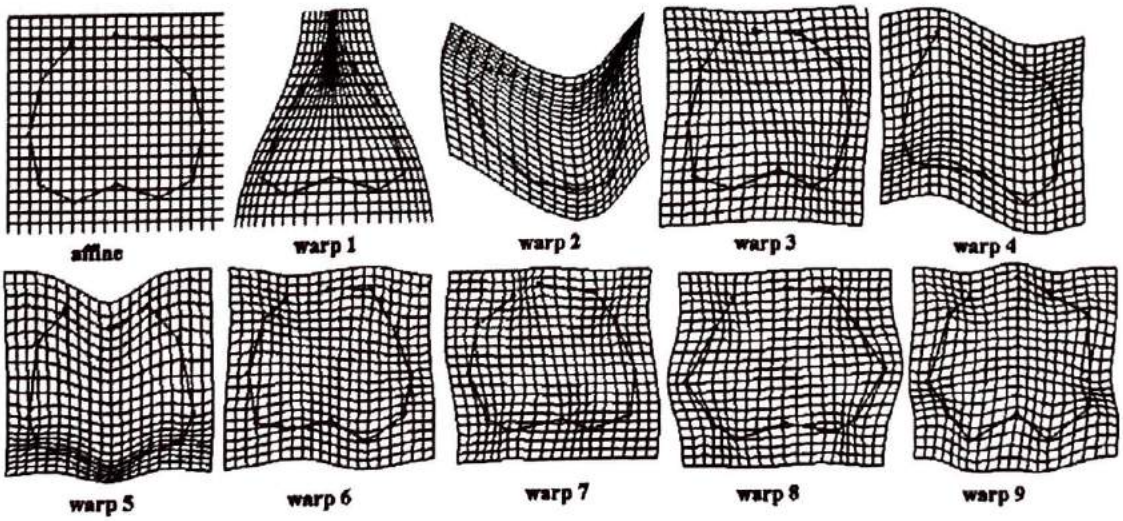

Figure 9. Affine (amplitude 0) or mean shape of the carapace and deformation grids of the nine partial warps shown at amplitude 10, the maximum amplitude that demonstrates the local deformation.

If the partial warp scores describe the pattern of local deformations of the specimens, relative warps are principal components that describe the major trends in shape variation within the overall sample. Because variation among the specimens is described in terms of the variance in the parameters of the spline function, expressed relative to the bending energy or Procrustes

distance matrices (Lynch *et al.*, 1996), both partial warps and relative warps are used in this study.

In relative warp analysis, the graphic representation allows to localize most expressed shape changes corresponding to a particular warp. It appears like an exaggerated illustration of the deformation so that the pattern along which direction the deformation exerts most visible change can be determined.

The relative warp, which corresponds to a principal component analysis (PCA) of the shape variation in tangent space using the weight matrix of partial warp scores, reduces the number of shape variables (partial warps) into a lesser number of more explanatory, independent shape vectors (Bookstein, 1982). These singular values (obtained by a single value decomposition of the weight matrix) are good representatives of the amount of variation explained by each relative warp. Figure 10 shows the first two relative warps used in the TPS reconstruction of shape variability of the carapace following a relative warp analysis.

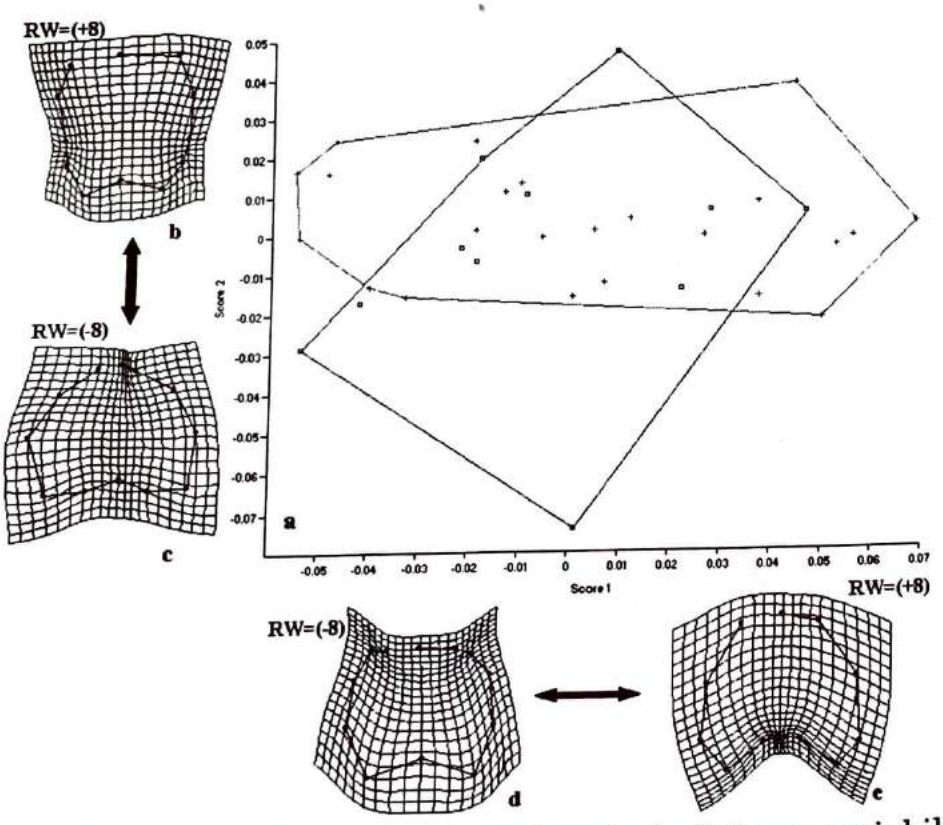

Figure 10. Thin-plate spline reconstruction (b-e) of shape variability along relative warp 1 (x-axis) and relative warp 2 (y-axis) following a relative warp analysis of the carapace. The original transformations are placed as points in the (a) PCA scatter plot (relative warp scores) providing a powerful data reduction technique for a set of transformations. Amplitude 8 best emphasizes the deformations where the variations are most expressed.

The original transformations are placed as points on the Principal Component Analysis (PCA) scatter plot on Figure 10a that provides a powerful data reduction technique for a set of transformations. In Figure 10a, the points that correspond to the males show extreme variations relative to warp 2 (along y- axis) while the females are mostly concentrated within the range of -0.02 to +0.03. This means that for the relative warp 2, the females mostly exhibit positive deviation that is characterized by the upward stretching of the anterior region and then compression of the postero-lateral sides that gives rise to the bulging of the dorsal carapace. This confirms the general observation using TPS visualizations that the carapace of females tend to be longer than wide, while that of the males are wider than long. Only 1 male, which is the specimen 2M, exhibited extreme negative variation that is characterized by the compression of the anterior region, the outward stretching of the lateral sides and the depression above landmark 6 along the mid-dorsal region. This is also the same male specimen that did not clump with the other males in the landmark plots in Figure 7a. All males and females exhibit varying deviation relative to warp 1 (x-axis). Positive deviation relative to warp 1 is characterized by the downward depression below landmark 6 and the outward and upward stretching of the anterior region whereas the negative variations relative to warp 1 are characterized by the outward stretching of the posterior region and the inward bending of the antero-lateral sides coupled by the downward compression of the anterior region. Amplitude 8 had been chosen for relative warp analysis because at this amplitude, the variation is most emphasized and the deformations that correspond to the shape variations along the transformation grids are best expressed.

Shape differences can be described by TPS that maps the deformation in shape from one specimen to another. The object is deformed or "warped" into another on the transformation grids. Differences in shapes among objects can then be described in terms of differences in the deformation grids depicting objects (Adams *et al.*, 2002). Shape differences in the sternal area have been analyzed with TPS and with warp functions, both of partial warps (Figures 11) and relative warps (Figure 12).

Transformation grids for partial warps 1 to 23 show varying degree and orientation of shape deformation. Different warps show different deformations such as folding (partial warps 2, 3, 6, 10, 11 18 and 19), bulging at the middle (partial warp 14) or at anterior region (partial warp 3), stretching or expansion (partial warps 3, 4, 6, 7, 13, 14, 16 and 17), compression (partial warps 1, 4, 5, 6, 7, 9, 10, 11, 13, 16, 17, 18, 19, 22 and 23), and in-between-landmark crumpling (partial warps 6, 8, 12, 14, 15, 17, 18, 20 and 21).

Of the 26 landmark points established on the sternal area of the ventral prosoma (Figure 3 and Table 3), the distance between landmarks 2 and 26, found along the medial plane at the base of the tritosternum had exhibited the greatest deformation. The bulging of the middle section or any stretching along the tritosternum area, the anterior region or even of the lateral regions

also affect landmarks 2 and 26, making them the most deformed points. The landmarks along the sides, such as landmarks 7, 8 and 9 at the left side and landmarks 19, 20 and 21 at the right side, have also exhibited a great degree of deformation.

It was observed that some males exhibit high scores for partial warp 2. This means that some males exhibit an inward folding of the lower left corner of the sternal area along the arbitrary diagonal line across the shape.

Of the partial warp scores of the males and females, the males are included within the range of the values of that of the females. This implies that the females exhibit greater diversity in the shape of the sternal area than the males.

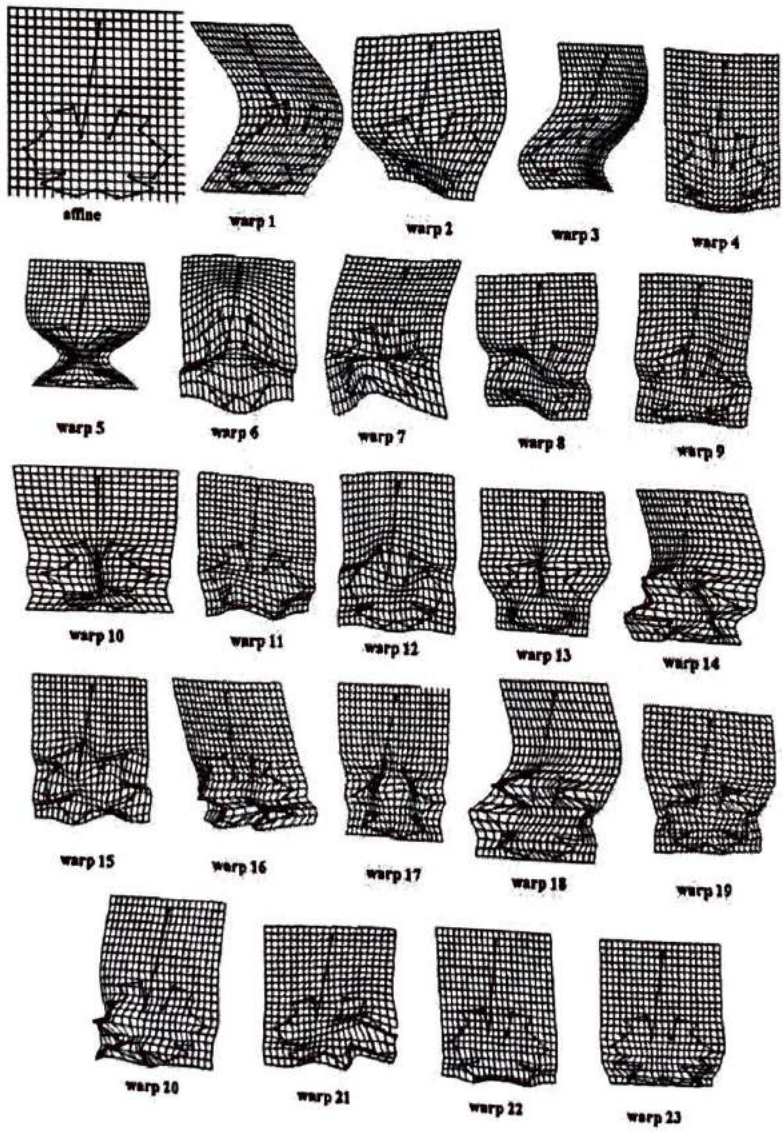

Figure 11. Affine (amplitude 0) or mean shape of the sternal area and deformation grids of the twenty-three partial warps shown at amplitude 10, the maximum amplitude that demonstrates the local deformation.

The principal component analysis of the coordinates of the landmark points of the sternal area was also carried out in the method of relative warps. Relative warps analysis of the two curves separately yield exactly the same conclusion about the groups that arose from the tests of Procrustes distance and the displays of Procrustes shape coordinates (Bookstein *et al.*, 1999). Figure 12 shows the TPS reconstruction of the two relative warps (corresponding for the first and second principal components) with overlapping relative warp scores for both the male and the female samples in the PCA scatter plot.

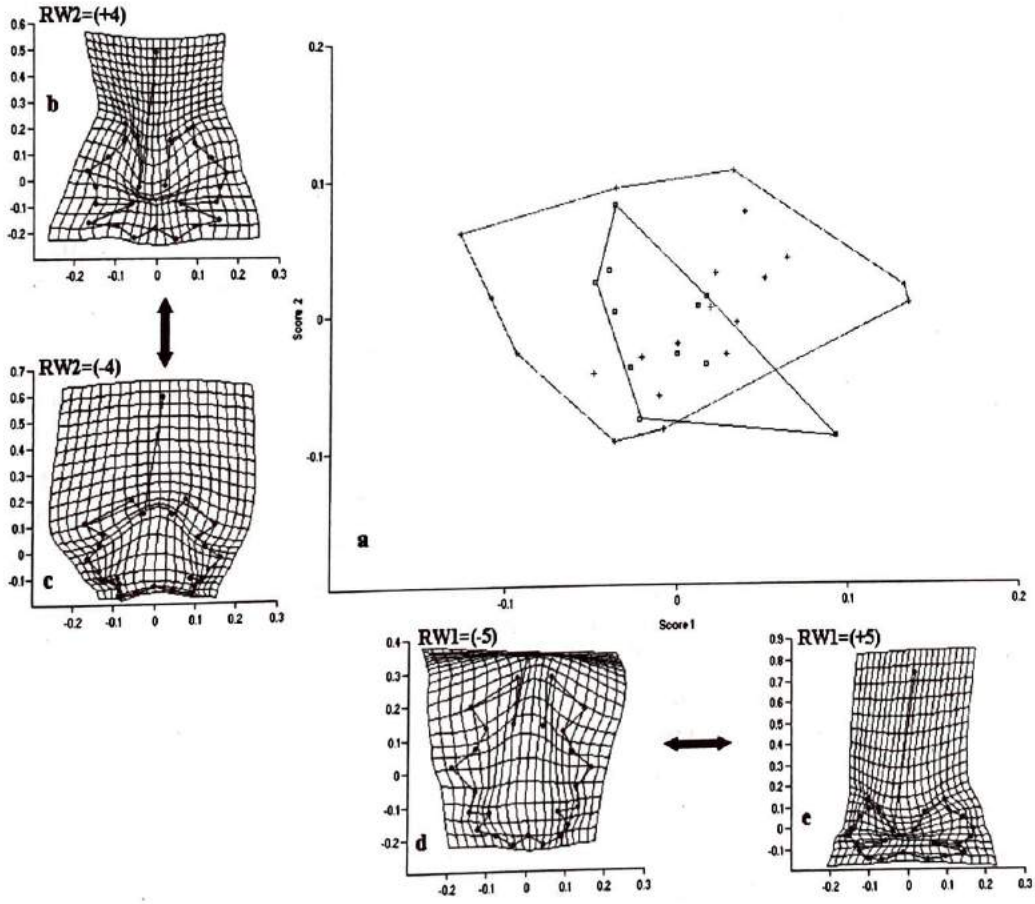

Figure 12. Thin-plate spline reconstruction (b-e) of shape variability along relative warp 1 (x-axis) and relative warp 2 (y-axis) of the sternal area following a relative warp analysis. The original transformations are placed as points in the (a) PCA scatter plot (relative warp scores) providing a powerful data reduction technique for a set of transformations. Amplitude 4 best emphasizes the deformations along warp 2 while amplitude 5 best expressed the shape variations relative to warp 1.

For the relative warp 2, positive deviations are inclined towards the downward compression of the sternal area such that a depression is formed on the mid-ventral section of the sternal area, along the base of the tritosternum (landmarks 2 and 26). Negative deviation of the relative warp 2 shows an upward stretching of the tritosternum region and the compression of the posterior region. Positive deviations for relative warp 1, on the other hand, show compression of the sternal area while the opposing negative deviation show the upward stretching of the sternal area. Both males and females exhibit similar range of deformations in terms of relative warp 2 but for the relative warp 1, the females exhibit greater shape diversity than the males as shown in the wider range of distribution in the PCA scatter plot of the relative warp scores of the sternal area.

Geometric morphometrics deals with shape deformations proper, so its ultimate aim, strictly speaking, is limited to Procrustes and partial warp scores that indicate to how one shape differs from others and to what extent do these shapes differ (Pavlinov, 2001). However, in this study, further analyses of the shapes of the carapace and the sternal area, such as the Principal Component Analysis (PCA), Hotelling's T^2 Test and Cluster Analysis were also applied using the PAleontological Statistics (PAST) software.

Shape differences were also evaluated using Multivariate Analysis of Variance (MANOVA) of the coordinate pairs, then summarized using canonical variates analysis (CVA) (Douglas *et al.*, 2001).

One-way MANOVA (Multivariate ANalysis Of VAriance) is the multivariate version of the univariate ANOVA that test whether several samples have the same mean (Hammer *et al.*, 2004). Here, two statistics were calculated: Wilk's Lambda (with associated Rao's F) and the Pillai trace (with its approximated F), the former being most commonly used but the latter is more robust (Hammer *et al.*, 2004). Both the Wilk's Lambda and the Pillai trace give significant p values, at 0.008419 and 0.007338, respectively, therefore the samples have the same mean. The one-way MANOVA of the carapace landmarks are shown on Table 6. The first significant eigenvalue (eigenvalue 1 = 13.2) contributes to the 99.98% variance of the carapace coordinates.

Table 6. Results of the one-way MANOVA using the landmark coordinates of the carapace.

Wilk's λ = 0.07024	Pillai trace = 0.9322
p value = 0.008419	*p* value = 0.007338
Eigenvalue 1: 13.2	Percent: 99.98
Eigenvalue 2: 0.0002311	Percent: 0.001751

The sternal area data was not subjected to MANOVA because the coordinates of the 26 landmarks exceeds the number of variables that can be run by the PAST software.

An option under MANOVA, canonical variates analysis (CVA) produces a scatter plot of specimens along the two first canonical axes, producing maximal and second to maximal separation between all groups (multigroup discriminant analysis), where the axes are the linear combinations of the original variables as in PCA (principal component analysis), and the eigenvalues indicate amount of variation explained by these axes (Hammer *et al.*, 2004). Figure 13 shows the CVA scatter plot of the carapace landmarks. Both male and female points overlap around 1000 of axis 1 and around zero of axis 2 (ranging from –200 to +100).

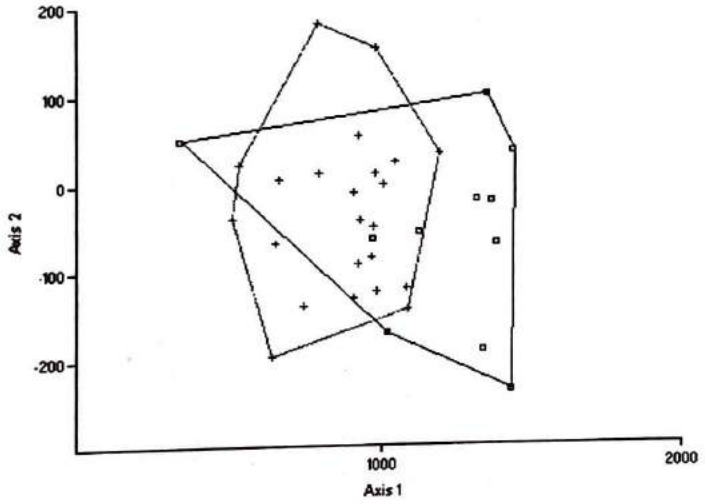

Figure 13. CVA scatter plot of the carapace landmark.

The PCA may be illustrated based on the loadings of the original variables to the reduced principal components. The loadings show to what degree the different *original variables* (given in the original order along the axis) enter into the different components. These component loadings are important in the interpretation the 'meaning' of the components (Hammer *et al.*, 2004). Figures 14 and 15 show the PCA loadings for the first significant principal component (component1). The values of the loadings are plot in the figures that show the amount of loading the variables (which are actually the x and y coordinates) that affected the variation of the carapace shape (Figure 14) and the direction of the deformation (Figure 15) from the mean shape with respect to the component.

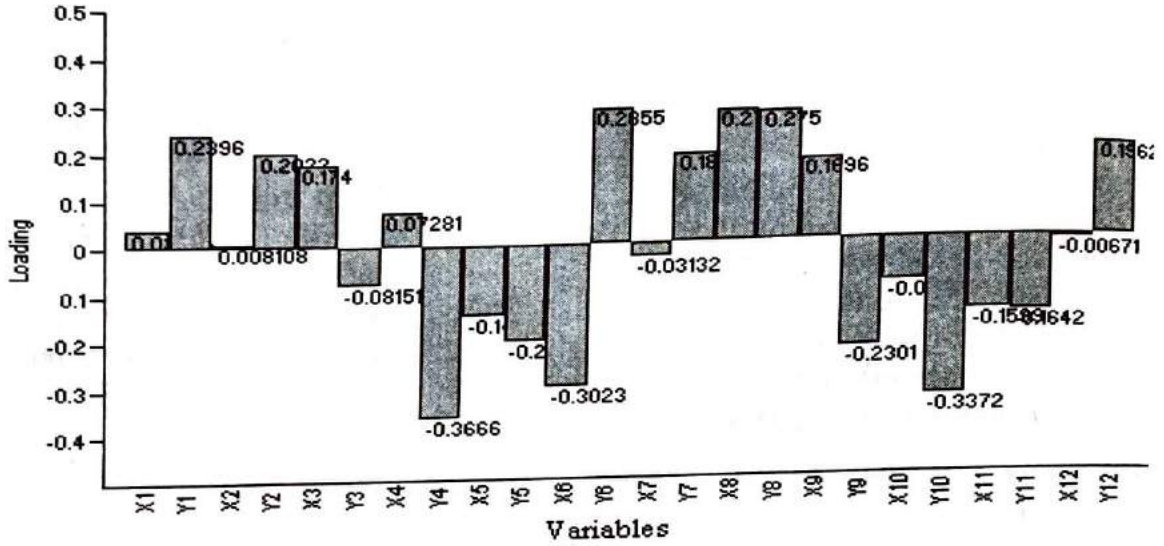

Figure 14. PCA loadings bar graphs for the first most significant components of the carapace landmarks.

The direction of the variations from the mean shape of the Procrustes fitted carapace landmark coordinates are shown by the displacement vectors in Figure 15. The direction of deviations is exhibited by the orientation of the lines that are connected to the landmarks points. For landmark 1, for instance, the deviation from the mean shape is going upwards and so if these were to be shown in the TPS, there will be an upward stretching in the vicinity of this landmark. The length of the lines shows the degree of deviation, such that landmark 7 is more greatly deviated from the mean than with landmark 1. The first component then is responsible for the deviation of the carapace shapes that make the carapace appear outwardly stretched towards the sides but coupled with downward compression of the grids, signifying depression of the lateral sides. Moreover, the upward direction of the displacement vectors at the anterior region of the carapace show that the component 1 is also responsible for the upward stretching of the anterior region of the carapace.

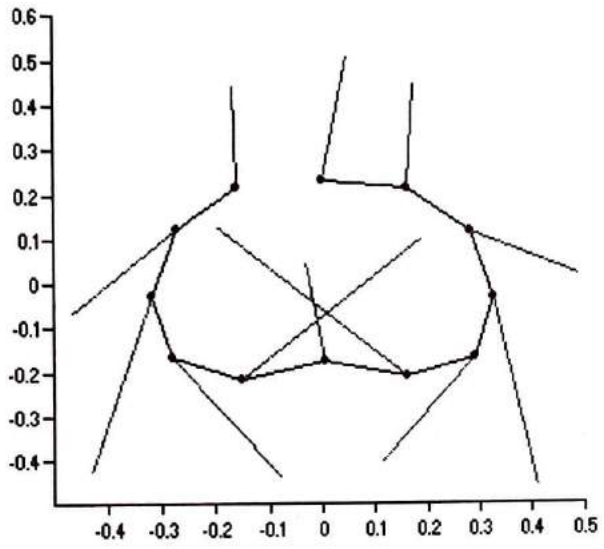

Figure 15. Displacement vectors corresponding to the first principal component that show the direction of deviation from the mean shape of the Procrustes fitted landmark coordinates.

The PCA loading values of the second significant components of the carapace are plot and illustrated as the bar graphs and displacement vectors in Figures 16 and 17, respectively.

In Figure 16, the coordinates X2 and X12 show the greatest loading of the second significant component relative to the positive and the negative deviations from the mean shapes of the carapace landmarks, respectively. Other variables, like X3, Y3, Y9 and X11 have also contributed much to the variation relative to the second significant component of the carapace shape.

Figure 17 shows that the second significant component or component 2 is responsible for the vertical elongation of the carapace such that most of the landmarks at the lateral and posterior regions are directed upwards (except for landmark 3 and 9 that have lines that are directed sideward and downward, respectively). The landmarks at the anterior region particularly landmarks 1, 2, 10 and 11 have lines that point downward and sideward. This implies that the second principal component is responsible for the elongation of the carapace shape making them appear longer than they are wide.

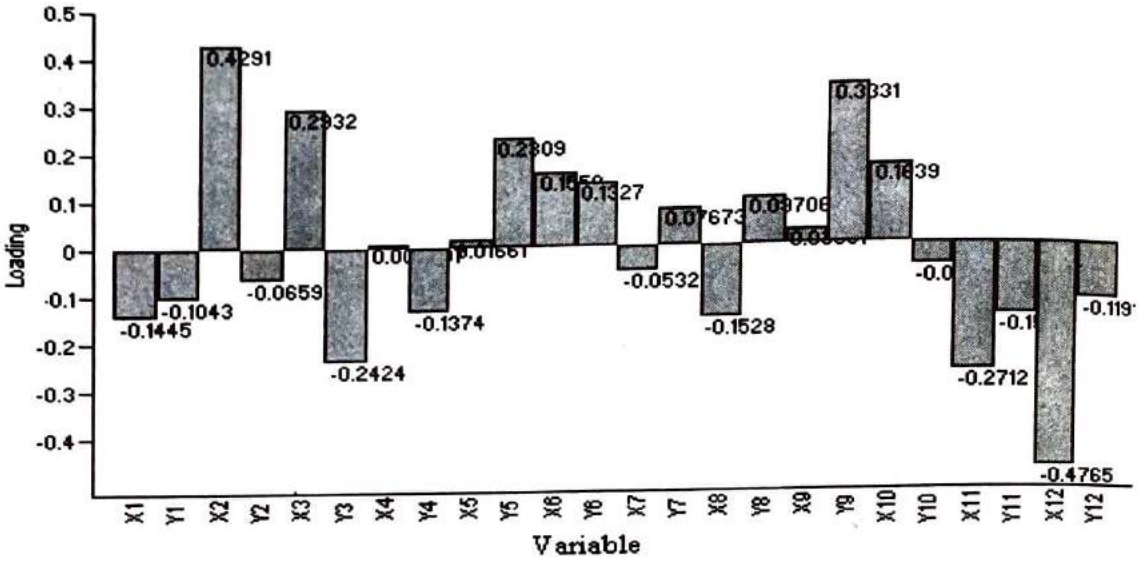

Figure 16. PCA loading for the second most significant component of the carapace landmarks.

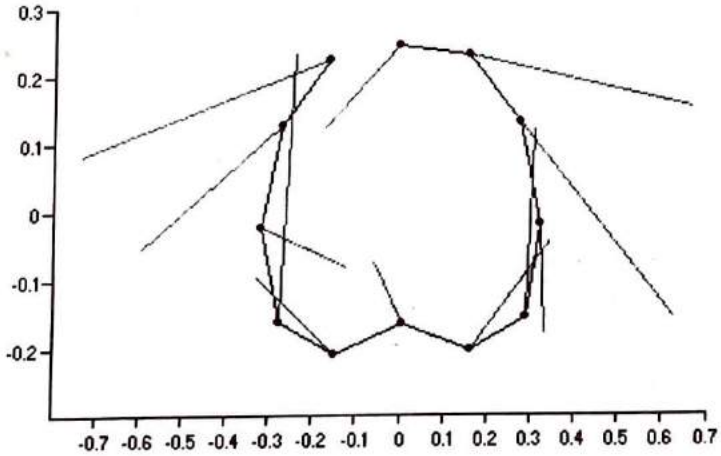

Figure 17. Displacement vectors from the mean carapace shape corresponding to the second principal component of the Procrustes fitted landmark coordinates.

The PCA loading values of the first significant component that are plot on a bar graph below (Figure 18) show that Y1 has the greatest loading value. When the loading values are plot using displacement vectors from the mean shape of the sternal area corresponding to the first principal component of the Procrustes fitted landmark coordinates (Figure 19), the longest line projecting downwards from landmark 1 shows the greatest deviation from the mean and so the tritosternum may be responsible for the greatest deformation. This is due to the varying length and orientation of the tritosternum relative to the oral cavity for the feeding process of the organism.

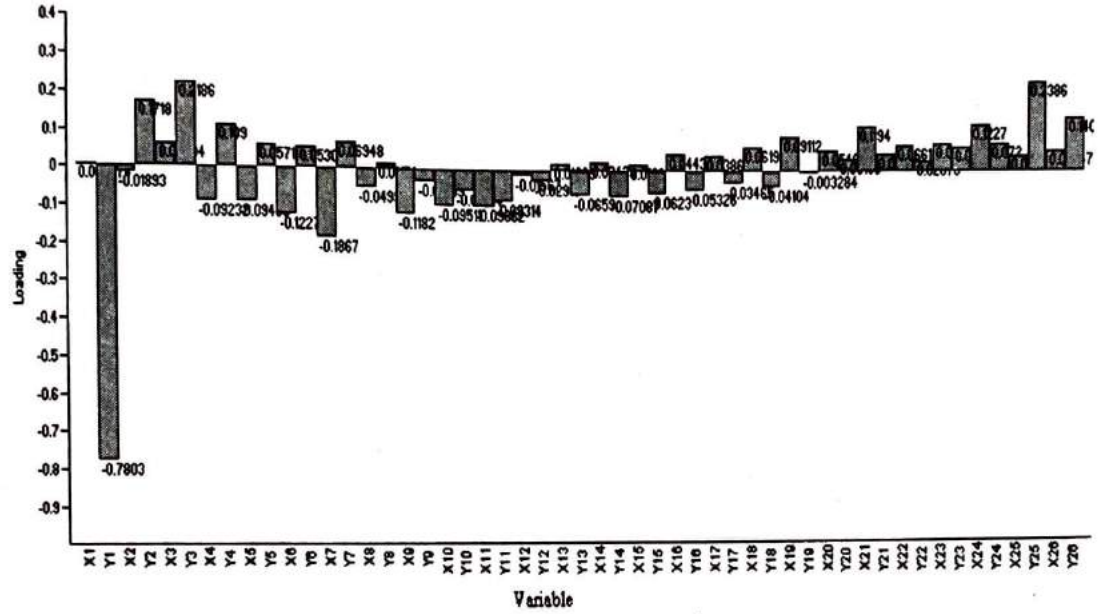

Figure 18. PCA bar graph loadings for the first significant component of the sternal area landmarks.

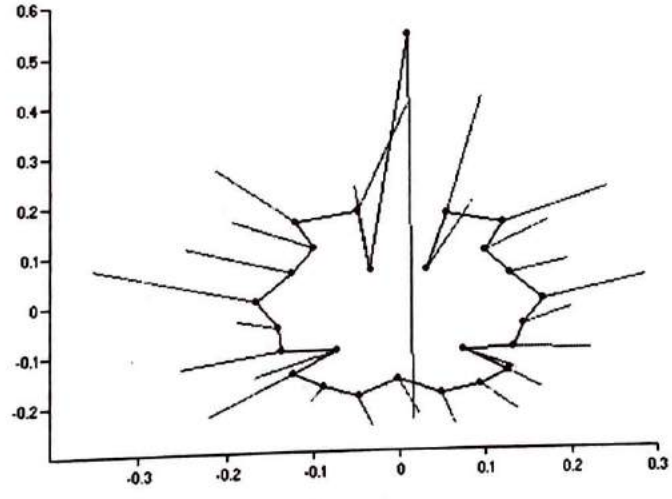

Figure 19. Displacement vectors from the mean shape of the sternal area corresponding to the first principal component of the Procrustes fitted landmark coordinates.

The PCA loading values of the second significant component are plot in a bar graph of the PCA loading (Figure 20) and the graph for the displacement vectors from the mean values (Figure 21). If the variation in component 1 is due to landmark 1 for the tritosternum, the component 2 is responsible for the between-landmark angular deformation of the sternal area. Landmarks Y2 and Y26 that are found at the base of the tritosternum account for most of the variation of the sternal shape.

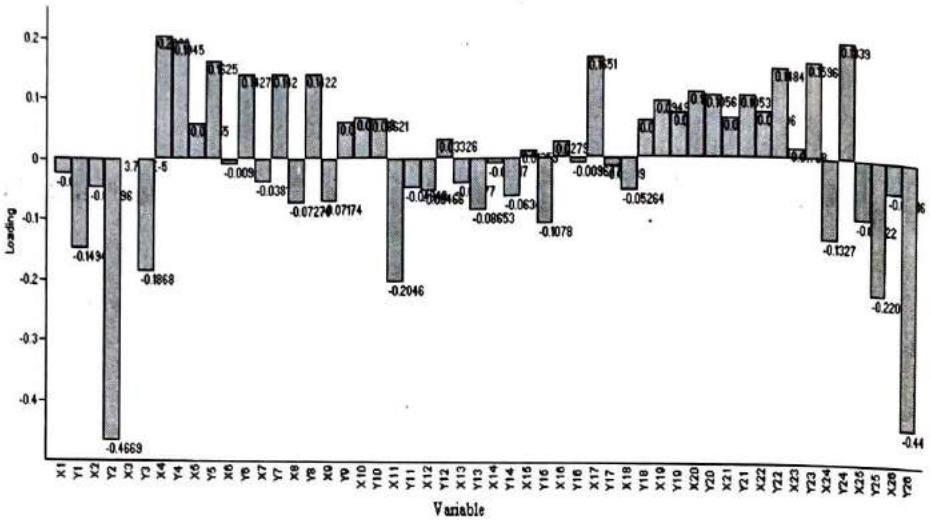

Figure 20. PCA bar graph loadings for the second significant component of the sternal area.

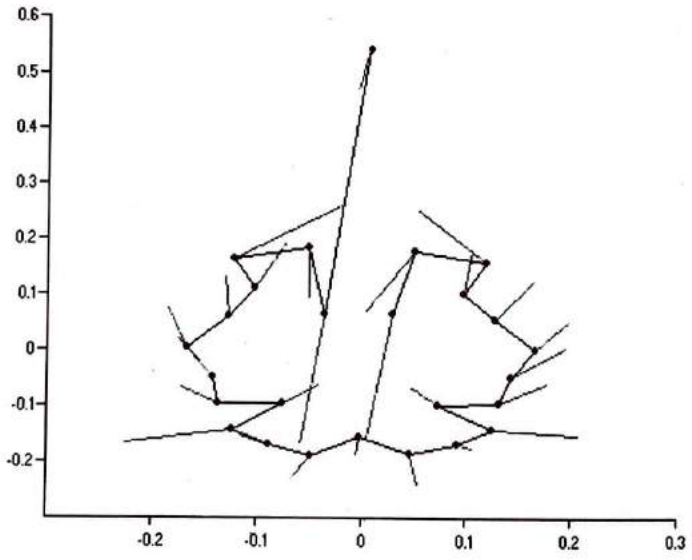

Figure 21. Displacement vectors from the mean shape of the sternal area corresponding to the second principal component of the Procrustes fitted landmark coordinates.

After subjecting the carapace and sternum landmarks to superposition and deformation methods, the third method, which is the linear-distance based method using the Euclidian Distance Matrix Analysis (EDMA), was applied.

The EDMA of the landmarks coefficients had been calculated from the distances between all pairs of landmarks using the PAST software. The number of pairs can be computed from N(N-1)/2 where N is the number of

landmarks (Hammer *et al.*, 2004). In this study, for instance, there were 66 pairs for the carapace and 325 pairs for the sternum.

Euclidean Distance Matrix Analysis (EDMA) has been considered as a solution to the limitations of the "coordinate-based" techniques (such as the TPS and the Procrustes) because EDMA is a "coordinate-free method" that is just based solely on the distances between landmarks and is invariant to rotation and translation of the original specimens (Lynch *et al.*, 1996; Hammer *et al.*, 2004). Multivariate analysis, like the PCA, had been applied on these EDMA values.

The PCA of the EDMA coefficients of the carapace gives three components with the corresponding eigenvalues and percentage variance summarized in Table 7. Principal component 1 accounts for 95.25% of the variance that means that the PCA of the carapace EDMA coefficients have been scored very successfully.

Table 7. Proportion of variation associated with the significant components using the EDMA coefficients of the carapace.

COMPONENTS	EIGENVALUES	%VARIANCE
1	3.426E+05	95.248
2	6.903E+03	1.9191
3	3.974E+03	1.1047

Figure 22 shows the PCA scatter plot of the EDMA coefficients with the overlapping values of the male and female specimens. Both male and female samples have similar range of distances relative to the second principal component along the y-axis. Relative to the x-axis, however, the males are mostly clumped at the range within 3000-4000 of the first significant component, but are widely dispersed relative to the second significant component. The female, then, show greater diversity in the carapace shape than the males.

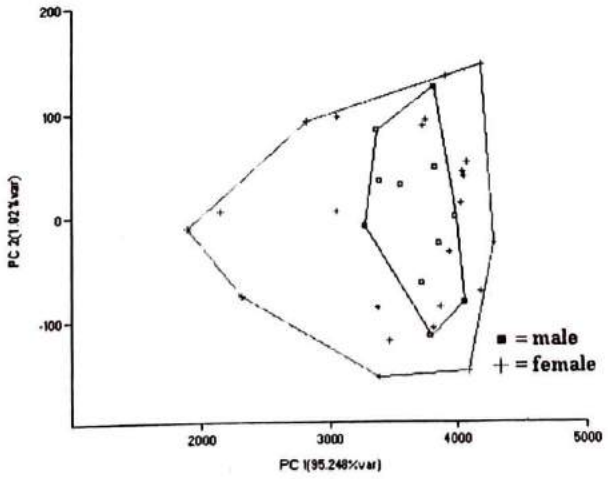

Figure 22. PCA Scatter plot using the EDMA coefficients of the carapace.

The proportion of variation associated with the significant components and the PCA scatter plot using the EDMA coefficients of the sternal area are shown in Table 8 and Figure 23, respectively. Table 8 shows that component 1 accounts for the percentage variance of 86.61%. This means that the PCA of the EDMA coefficients of the sternal area had been scored successfully.

Table 8. Proportion of variation associated with the significant components using the EDMA coefficients of the sternal area.

COMPONENTS	EIGENVALUES	%VARIANCE
1	1.247E+05	86.611
2	8.896E+03	6.180
3	2.325E+03	1.615
4	2.079E+03	1.445
5	1.628E+03	1.131
6	7.204E+02	0.500
7	5.985E+02	0.416
8	4.970E+02	0.345
9	4.482E+02	0.311
10	3.588E+02	0.249

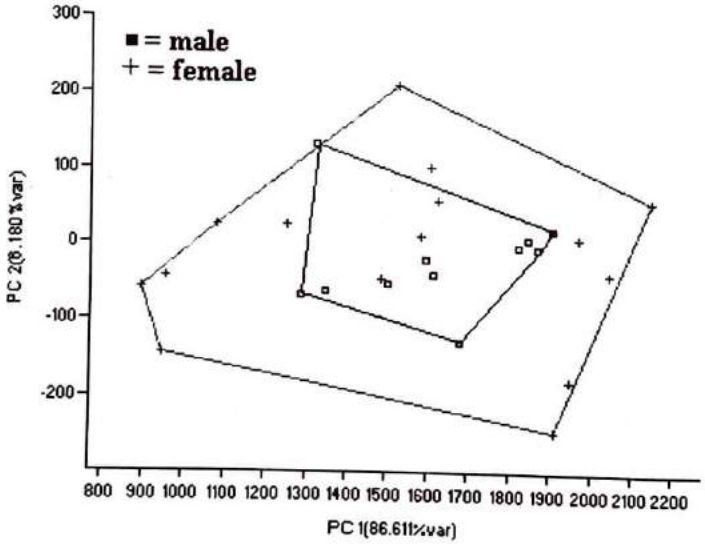

Figure 23. PCA Scatter plot of the sternal area using the EDMA coefficients.

Another multivariate method applied as landmark analysis in this study is Hotelling's T^2 Test. The typical application of Hotelling's T^2 is the testing for separation and equal means of two multivariate data sets with the assumption for multivariate normality and equal covariances (Hammer *et al.*,

2004). Given the two sets of coordinates for each landmark, using PAST software, an axis is constructed which maximizes the difference between the sets that are then plotted along this axis using a histogram (Figures 24 and 25). Based on the given p values for the test of means of the carapace and the sternal area, the carapace did not give significant p at 0.2448 so the carapace landmark means are not equal. On the other hand, the p value of the Hotelling's test for sternum is equal to zero, so the means of the landmarks of the sternal area are equal.

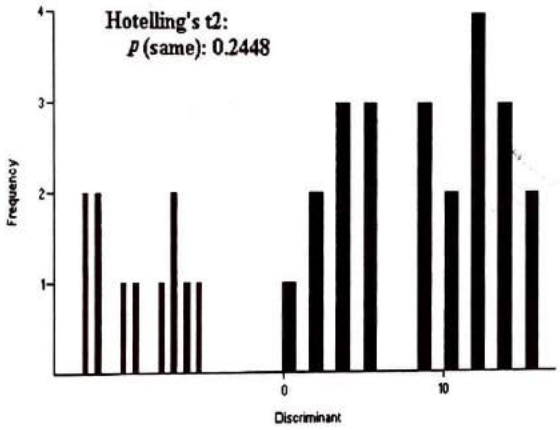

Figure 24. Frequency distribution of the component scores of the carapace of the individuals showing the male specimens (blue) and the female specimens (red).

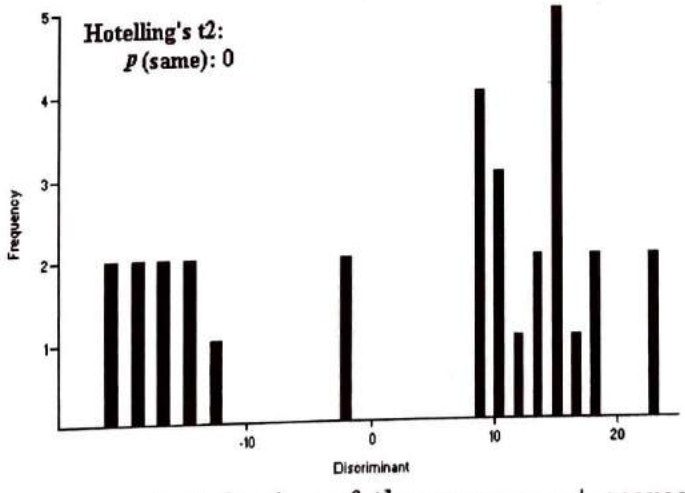

Figure 25. Frequency distribution of the component scores of the sternal area of the individuals showing the male specimens (blue) and the female specimens (red).

The term *cluster analysis* encompasses a number of different algorithms and methods for grouping objects of similar kind into respective categories. The Cluster analysis does not mention anything about statistical significance testing. In fact, cluster analysis is not as much a typical statistical test as it

is a "collection" of different algorithms that "put objects into clusters according to well defined similarity rules" (Hammer *et al.*, 2004). The hierarchical clustering produces a dendrogram or phenogram (Figures 26 and 27) based the clustering algorithm used.

Ward's method is algorithm used in this study. It is distinct from all other methods because it uses an analysis of variance approach to evaluate the distances between clusters. In short, this method attempts to minimize the Sum of Squares (SS) of any two (hypothetical) clusters that can be formed at each step. With this method, clusters are joined such that increase in the within group variation is minimized (Hammer *et al.*, 2004). In general, this method is regarded as very efficient; however, it tends to create clusters of small size(Hammer *et al.*, 2004).

Figures 26 and 27 show the unweighted phenogram of the male and female specimens based the shapes of their carapace and sternal area, respectively. The two figures show heterogeneous clustering, with the males widely mixed with the females. Both phenograms show specimen 2M at the topmost spot, separated from the other samples, as an outlier in Figure 26 but as one distinct specimen under the same clade with 20F and 23F in Figure 27. Being an outlier based on its carapace shape is expected of specimen 2M because it has also deviated from the group of males in the landmarks plot in Figure 7.

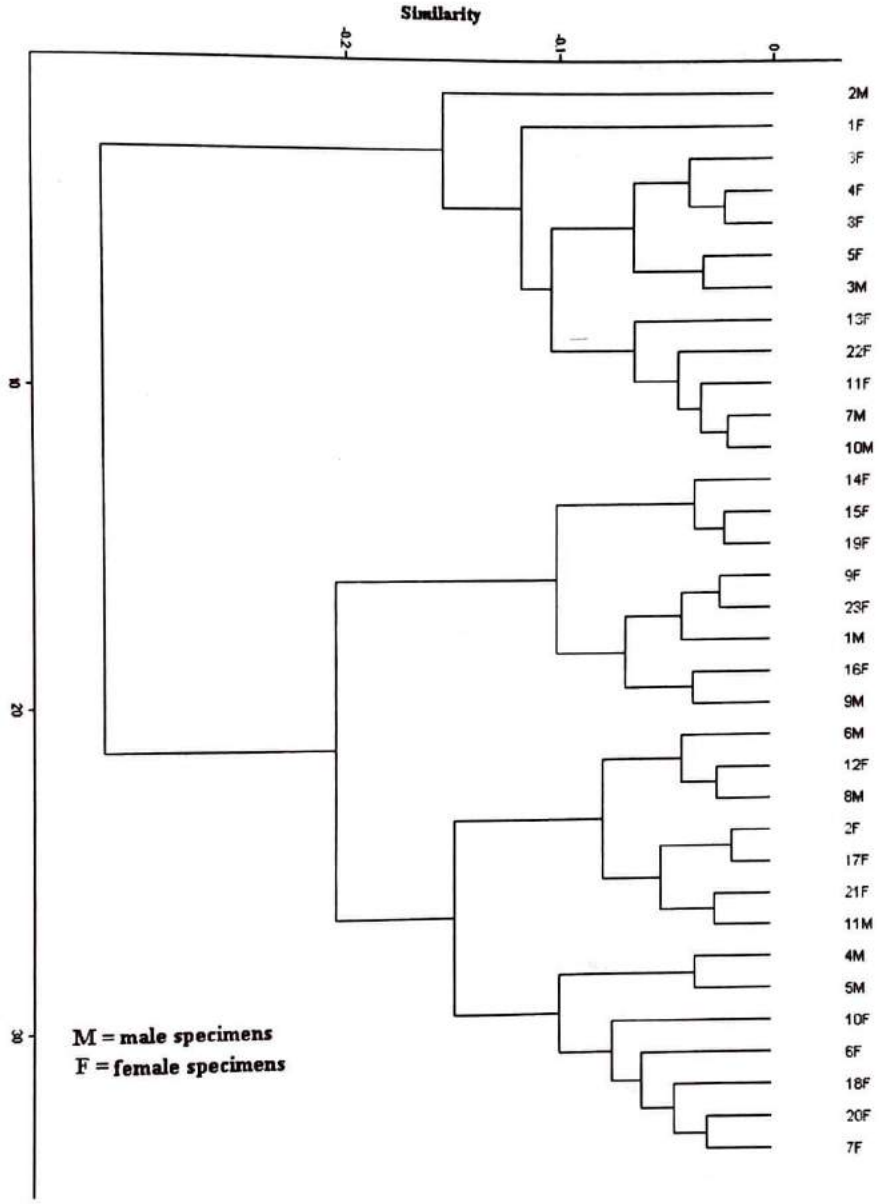

Figure 26. Unweighted Phenogram of the carapace of the male and female specimens based on clustering of a matrix using Ward's method algorithm.

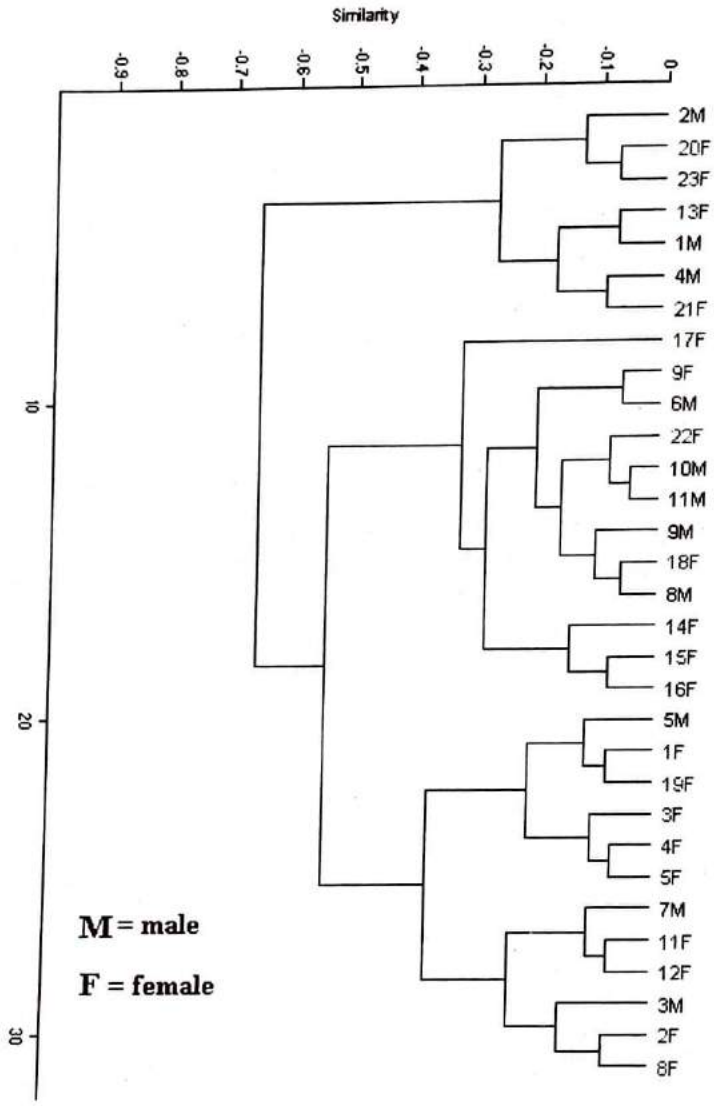

Figure 27. Unweighted Phenogram of the sternal area in male and female specimens based on clustering of a matrix using Ward's method algorithm.

One limitation of the landmark-based geometric methods is that a sufficient number of landmarks may not be available to capture the shape of the structure. Many authors consider outline methods as valid and important morphometric approach and classify them together with landmark-based geometric morphometric methods. It is for this reason that in most geometric studies, both the landmark and outline methods are applied, just like in this study.

An outline is mathematical curve that stands for the image of a physical boundary of an object and the outline data can be archived as a sequence of point coordinates (Adams *et al.*, 2002). The x and y coordinates of the outline points on the carapace and on the ventral opisthosoma are recorded and analyzed in this study.

The x and y coordinates of the 44 outline points on the carapace and the 56 outline points on the ventral opisthosoma were analyzed using elliptic Fourier shape analysis (EFA) and Eigenshape Analysis (EA). Outlines of structures can be captured and analyzed using shape variables such as those generated by an EFA. By far, EFA is the most commonly used strategy for analysis of outlines is to fit some trigonometric, polynomial, or spline functions. The coefficients derived from the fit are then used as morphometric variables and analyzed using standard multivariate methods such as PCA (Smith and Bunjie, 1999). Figures 28 and 29 show the graphical representation of shapes of the carapace of female and male whip spiders based on elliptic Fourier shape analysis.

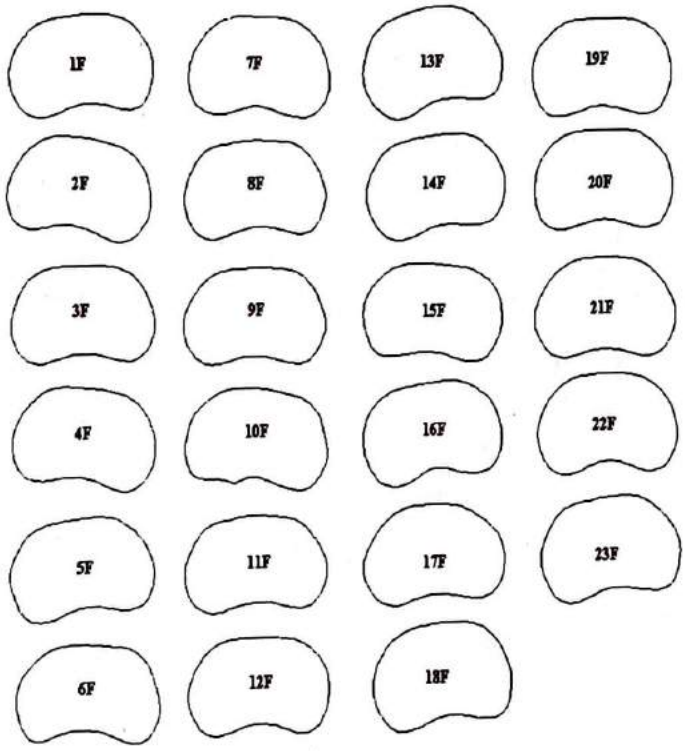

Figure 28. Graphical representation of shapes of the carapace of female specimens based on elliptic Fourier shape analysis.

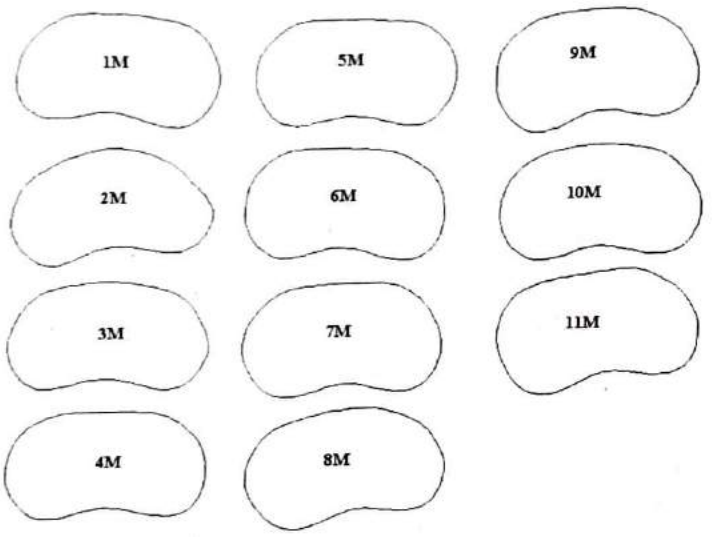

Figure 29. Graphical representation of shapes of the carapace of male specimens based on elliptic Fourier shape analysis.

The coefficients of the 12 landmark points were analyzed using PCA. Table 9 shows three components with the first significant component having a very high % variance of 95.543. Because most of the variance are accounted for by the first principal component, the PCA of the EFA coefficients have been scored successfully.

Table 9. Proportion of variation after PCA using the EFA coefficients of the carapace outline points.

COMPONENT	EIGENVALUES	%VARIANCE
1	1.934E-02	95.543
2	3.099E-04	1.531
3	2.078E-04	1.026

The resultant elliptic Fourier coefficients of the carapace outline points shown on the PCA scatter plot in Figure 30 do not exhibit distinct groupings of the male and female amblypygids. There is overlapping of the male and female elliptic Fourier coefficients, so based on the carapace outline, the specimens did not exhibit sexual dimorphism.

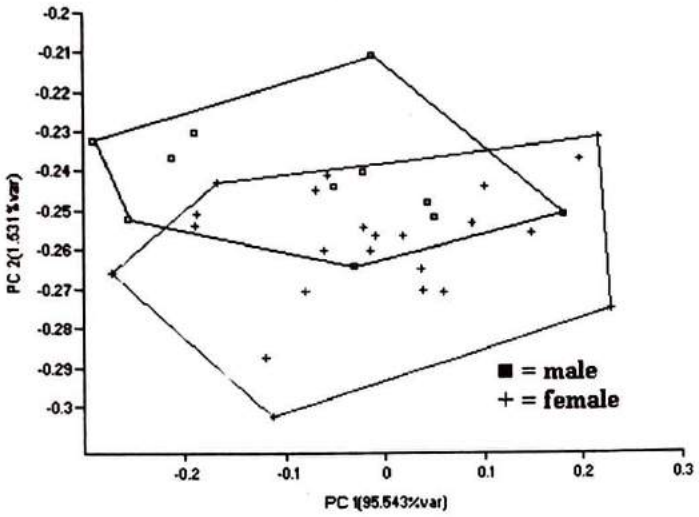

Figure 30. PCA scatter plot of the resultant elliptic Fourier coefficients of the carapace outline points.

Figures 31 and 32 show the graphical representation of shapes of the opisthosoma of female specimens based on elliptic Fourier shape analysis. Compared to the graphical representation of the carapace outlines in Figures in 31 and 32, the outlines of the opisthosoma show obvious differences on their shapes, lengths, widths and orientation for both the male and the female specimens, but the most obvious shape differences, are exhibited by the female whip spiders. The females exhibit greater carapace shape diversity than the males.

Based on Figure 31, different shapes, contours and orientations of the graphical representation of the opisthosomal shapes can be observed. For example, 4F and 12F are much more rounded that the 13F and 19F. These latter two, as well as 14F, seem to be inclined towards the left in contrast to 16F that is rather inclined slightly towards the right.

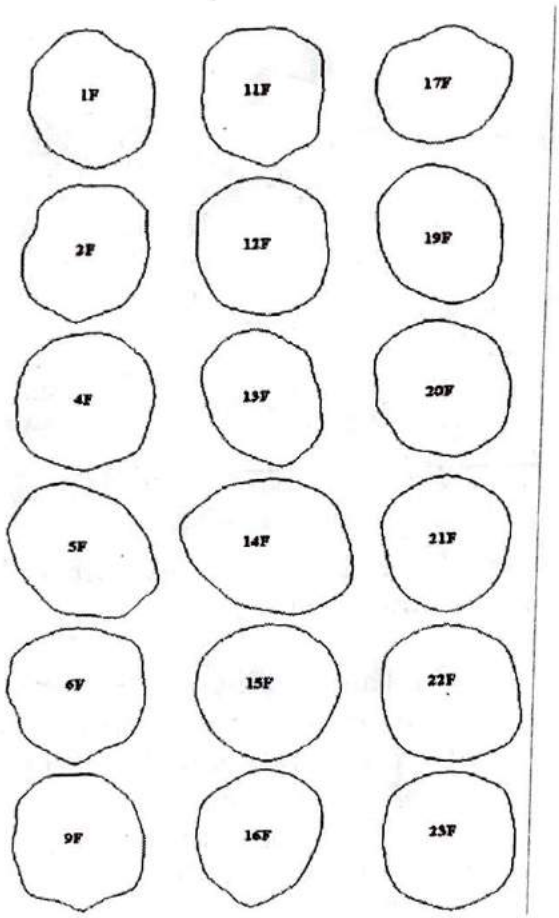

Figure 31. Graphical representation of shapes of the opisthosoma of female specimens based on elliptic Fourier shape analysis.

The male specimens in Figure 32 also show differences in shape and contour of their opisthosoma but not as varied as those of the females.

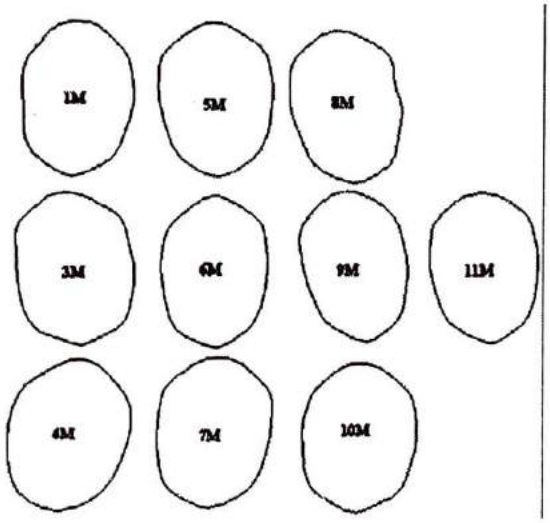

Figure 32. Graphical representation of shapes of the opisthosoma of male specimens based on elliptic Fourier shape analysis.

The coefficients of elliptic Fourier analysis of the opisthosomal outline when analyzed using PCA give the summary of 3 components (Table 10) with the first significant component having a % variance of 87.002. The second component follows with only 8.5% of the variance. So, since most of the variance are accounted for by the first principal component, the PCA of the EFA of the opisthosomal shape has been scored successfully. Therefore, the components with the corresponding eigenvalues are significant.

Table 10. Proportion of variation after PCA using the EFA coefficients of the opisthosoma outline points.

COMPONENT	EIGENVALUES	%VARIANCE
1	1.876E-02	87.002
2	1.842E-03	8.539
3	2.532E-04	1.174

The PCA scatter plot of the resultant elliptic coefficients of the outline points of the opisthosoma (Figure 33) shows that the males form a cluster where their values are close to each other around the 0.60 to 0.65 mark along the y-axis that corresponds to the second principal component and around zero to 0.4 range relative to the first principal component along the x-axis. Although most of the values of the females also fall around the cluster of the males, the females show widely distributed values of the elliptic Fourier coefficients thus exhibiting a greatly dispersed distribution within the PCA

scatter plot. Based on the outline of the ventral opisthosoma, the females still exhibit greater diversity in shape than the males sampled in this study.

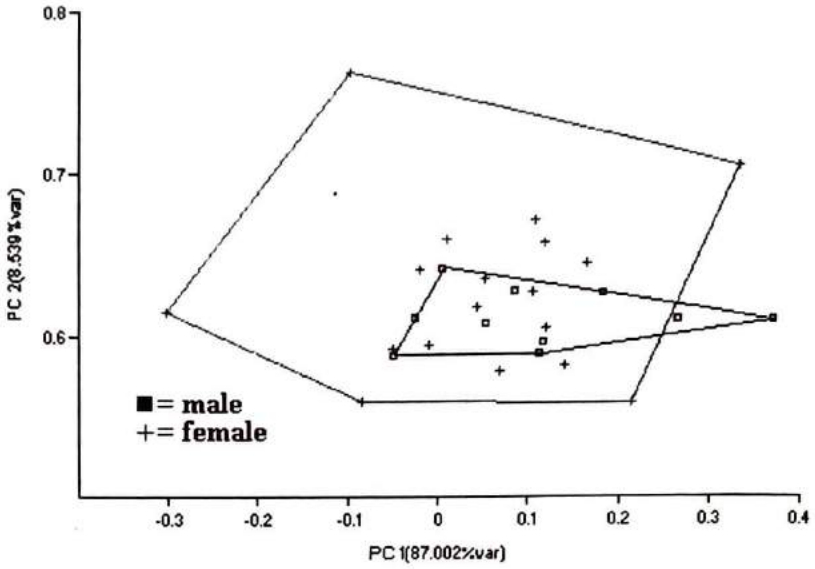

Figure 33. PCA scatter plot of the resultant elliptic Fourier coefficients of the outline points on the ventral opisthosoma.

Conclusions and Recommendations

The whip spiders sampled from Initao National Park, Initao, Misamis Oriental are believed to be under a new species of amblypygids under the genus *Charon* of Family Charontidae because they exhibit unique species-specific characteristics based on the number of articles on the tibia and tarsus of the first pair of legs and on the spination formula of their pedipalps. Of the 72 characters measured in the fluctuating asymmetry (FA) study of this research, only three traits, namely characters 44, 45 and 62 that correspond for leg 3 femur length, leg 3 patellar length and leg 4 basitibia 3 length, respectively, exhibit characteristics that can be considered as most ideal after all the series of tests done. Geometric morphometric analyses on the landmarks of the dorsal carapace and the sternal area as well as on the outlines of the carapace and the opisthosoma show that the females exhibit greater shape diversity than the male samples.

In the future studies, it is desirable to increase the number of samples of both the male and female specimens, as well as to compare the samples from Initao National Park with the previously identified type specimens belonging to the other species under genus *Charon,* with the original type specimens collected by Gervais from the Philippines (1842) and with those specimens collected by Weygfoldt (2002) in order to identify whether the samples merit a new species status based on international standards.

Biochemical and cytogenetic tests, the growth and developmental mechanisms of the whip spiders, their genetic effects, and the examination of

the genitalia, of the other internal organs and of the minute external structures such as the trichobothria, are among the research gaps that can still be filled in about the study of the amblypygids collected from Initao National Park, Misamis Oriental, Philippines.

References Cited

Adams, D. C., F. J. Rohlf and D. E. Slice. "Geometric Morphometrics: Ten Years of Progress Following the 'Revolution'". Web of Science. 2002. Online. January 29, 2004. http://www.public.asu.edu/`jmlynch/geomorph/index.html.

Anne, P., F. Mawri, S. Glastone and D. C. Freeman. 1998. Is Fluctuating Asymmetry a Reliable Biomonitor of Stress? A Test Using Life History Parameters in Soybean. Int. J. Plant Sci. 159(4): 559-565.

Bookstein, F. L. 1982. Foundations of Morphometrics. Ann. Rev. Ecol. Syst. 13:451-470.

Bookstein, F. *et al.*, 1999. Comparing Frontal Cranial Profiles in Archaic and Modern *Homo* by Morphometric Analysis. The Anatomical Record (New Anat.), 257:217-224.

Brignoli, P. M. 1973. Ragni delle Filippine, I. Un nuovo *Althepus* cavernicolo dell Isola di Mindanao (Araneae, Ochyroceratidae). Int. J. Speleol.5: 111-115.

Douglas, M. E., M. R. Douglas, J. M. Lynch and D. M. McElroy. 2001. Use of Geometric Morphometrics to Differentiate *Gila* (Cyprinidae) within the Upper Colorado River Basin. Copeia 2: 389-400.

Farlex, Inc. "Amblypygi". The Free Dictionary dot Com Website. 2004. Online. November 11, 2004. http://encyclopedia.the freedictionary.com/Amblypygi.

Frederick, S. H. "Scion Image for Windows". Scion Corporation. 2000. Online. October 23, 2005. http://www.scioncorp.com.

Gervais, M. P. 1842. Entomologie. L'Institut, Journal Universel Des Sciences et des Societes Savantes en France et a L'Etranger, 1'ere Section. 10:76.

Graham, J. H., D. C. Freeman and J. M. Emlen. 1993. Antiasymmetry, Directional Asymmetry, and Dynamic Morphogenesis. Genetica 89: 121-137.

Graham, J. H., D. C. Freeman and J. M. Emlen. 1993. Developmental Stability: A Sensitive Indicator of Populations under Stress. *Environmental Toxicology and Risk Assessment*. W. G. Landis, J. S. Hughes and M. A. Lewis, eds. American Society for Testing and Materials, pp. 136-158.

Graham, J. H., J. M. Emlen and D. C. Freeman. 1993. Developmental stability and its Applications in Ecotoxicology. Ecotoxicology 2: 175-184.

Hammer, O. "Morphometrics – brief notes". PAST Online. July 15, 2002. Online. September 21, 2004. http://folk.uio.no/ohammer/morphometrics

Hammer, O, D.A.T. Harper and P. D. Ryan. "PAST- PAleontological STatistics ver. 1.27". PAST Online. July 15, 2004. Online. October 23. 2004. http://folk.uio.no/ohammer/past

Harvey, M. S. and P. L. J. West. 1998. New Species of *Charon (Amblypygi, Charontidae)* From Northern Australia and Christmas Island. Journal of Arachnology. 26:273-284.

Harvey, M. S. 2002. The First Old World Species of Phrynidae (Amblypygi); *Phrynus exsul* from Indonesia. Journal of Arachnology 30:470-474.

Harvey, M. S. 2002. The Neglected Cousins: What Do We Know about the Smaller Arachnid Orders? Journal of Arachnology 30:357-372.

Juberthie, C. and V. Decu. nd. Philippines. Vol. 1. Societe de Biospeologie, Moulis and Bucarest. pp. 1957-1970.

Lynch, J. M., C. G. Wood and S. A. Luboga. 1996. Geometric Morphometrics in Primatology: Craniofacial Variation in *Homo sapiens* and *Pan troglodytes*. Folia Primatol 67: 15-39.

Oxnard, C. E. 1978. One Biologist's View of Morphometrics. Ann. Rev. Ecol. Syst. 9: 219-241.

Palmer, A. R. 1994. Fluctuating Asymmetry Analyses: A primer, pp.335-364. *In* T. A. Markow (ed.) *Developmental Instability: Its Origins and Evolutionary Implications*. Kluwer, Dordrecht, Netherlands.

Pavlinov, I. Ya. "Geometric Morphometrics, a New Analytical Approach to Comparison of Digitized Images". Moscow M. V. Lomonosov State

University Website. June 22, 2001. Online. January 29, 2004. http://www.zoomuz.bio.msu.ru. ///H|/Pavl/Pavlinov's_text.htm.

Pretre, J. G. and Forestier. (1816-1830). "Dictionaire des Sciences Naturelles". (poster/illustration).

Raffray, A., J. Bolivar and E. Simon. 1892. Voyage de M.E. Simon auz iles Philippines. Arthropodes cavernicoles de l'ilede Luzon. Coleopteres par. Raffray A. 61:28-29. Orthopteres par Bolivar MJ; 61-29-34. Ann. Soc. Ent. France 61:27-28

Richtsmeier, J. T., V. B. De Leon and S. R. Lele. 2002. The Promise of Geometric Morphometrics. Yearbook of Physical Anthropology 15: 63-91.

Rohlf, F. J. 2002. Geometric Morphometrics in Systematics. Published as Chapter 9 in N. Macleod and P. Forey (eds.) *Morphology, shape and phylogenetics*. Taylor & Francis: London. Pp. 175-193. Also available in acrobat format as "Geometric Morphometrics and Phylogeny". 2000. Online. January 29, 2004. http://life.bio.sunysb.edu/ee/rohlf/reprints/reprints.html.

Rohlf, F. J. and L. F. Marcus. 1993. A Revolution in Morphometrics. TREE 8(4): 129-132.

Simon, E. 1892. *Arachnides des iles Philippines*. Ann. Soc. Entomol. France 61: 35-52.

Smith, L.H. & Bunjie, P.M. 1999. Elliptic Fourier Analysis. *Paleobiology*, **25:** 396-408.

Weygoldt, P. 1999. Spermatophores and the Evolution of Female Genitalia in Whip Spiders (Chelicerata, Amblypygi). Journal of Arachnology 27: 103-116.

Weygoldt, P. 2000. Whip Spiders, (Chelicerata, Amblypygi), Their Biology, Morphology and Systematics. 163pp., Apollo Books, Stenstrup, Denmark.

Weygoldt, P. 2002. Sperm Transfer and Spermatophore Morphology of the Whip Spiders *Sarax buxtoni, S. brachydactylus* (Charinidae), *Charon* cf. *grayi*, and *Stygophrynus brevispina* nov. spec. (Charontidae) (Chelicerata, Amblypygi). Zoologischer Anzeiger 241: 131-148.